Electronic Supplementary Material (ESI) for New Journal of Chemistry

Electronic Supplementary Information (ESI)

A new fluorescent hemicryptophane for acetylcholine recognition with an unusual recognition mode

Nicolas Fantozzi,[a] Rémi Pétuya,[b] Alberto Insuasty,[c] Augustin Long,[c] Sara Lefevre,[d] Aline Schmitt,[d] Vincent Robert,[e] Jean-Pierre Dutasta,[d] Isabelle Baraille,[b] Laure Guy,[d] Emilie Genin,[a] Didier Bégué,[b] Alexandre Martinez,[c] Sandra Pinet*[a] and Isabelle Gosse*[a]

[a] Université Bordeaux, CNRS, Bordeaux INP, Institut des Sciences Moléculaires, UMR 5255, F-33400, Talence, France

[b] Université de Pau et des Pays de l'Adour, E2S UPPA, CNRS, IPREM, Institut des Sciences Analytiques et de Physicochimie pour l'Environnement, UMR5254, Pau, France.

[c] Aix Marseille Univ., CNRS, Centrale Marseille, iSm2, UMR 7113, 13397, Marseille, France

[d] Laboratoire de Chimie, École Normale Supérieure de Lyon, CNRS, UCBL, 46 allée d'Italie, F-69364 Lyon, France

[e] Laboratoire de Chimie Quantique, Institut de Chimie, UMR UDS-CNRS 7177, Université de Strasbourg, Institut Le Bel, 4, rue Blaise Pascal, F-67000 Strasbourg, France.

Table of contents

1. General information

NMR spectra were recorded on either a Bruker Avance 300 or a Bruker Avance 600 spectrometer. Chemical shifts are reported using the residual solvent peak as internal reference for ^{1}H or for ^{13}C.

HRMS (ESI-MS) were performed on various mass spectrometers. A Waters SYNAPT G2 HDMS mass spectrometer with an atmospheric pressure ionization (API) source was used for the mass spectra of compounds **4** and **5**. Agilent 6560 mass spectrometer was used in case of compounds **1**. Spectra were obtained with TOF analysis. A Q Exactive Hybrid Quadrupole-Orbitrap mass spectrometer was used for the analysis of **6**.

Steady-state absorption spectra were recorded between 200 nm and 500 nm on a Varian Cary 100 Scan spectrophotometer, using a quartz cuvette (1 cm x 1 cm x 4.5 cm).

Photoluminescence spectra were collected with a Varian Eclipse fluorescence spectrophotometer. The emission spectrum (λ_{exc} = 319 nm) was recorded between 328 nm and 450 nm with a maximum at 354 nm. All the emission spectra were corrected. Emission quantum yield was determined by using quinine sulfate as reference standard, which has a known emission quantum yield of 0.65 in 0.5 M sulfuric acid.[1] The reported fluorescence quantum yield is within ±10%. In the titration experiments guest aliquots were added with a microsyringe to a $2x10^{-5}$ M solution of **1** in chloroform containing 2% of methanol, placed in the fluorimeter cell at 20°C. After each guest addition, the cell was stirred for 2 min before recording the emission spectrum. Integrated signals rather than peak heights were used in the titrations. The volume change due to the additions is taken into account in the calculation. Measurements were repeated to verify their reproducibility.

Photoluminescence emission (A/A_0), based on the titration data, represents the PL emission area of the probe in the presence of the guest (A) normalized to the initial PL emission area (A_0) in the absence of the anion. Time-resolved fluorescence measurements were performed on dilute solutions (ca. 10^{-6} M, optical density 0.1) in standard 1 cm quartz cuvettes using an Edinburgh Instruments (FLS920) spectrofluorimeter in photon-counting mode. Fluorescence lifetimes were measured by time-correlated single-photon counting (TCSPC) using the same FLS920 spectrofluorimeter. Excitation was achieved by a hydrogen-filled nanosecond flash lamp (repetition rate 40 kHz). The instrument response (FWHM ca. 1 ns) was determined by measuring the light scattered by a Ludox suspension.

For the determination of formation constants, the spectrophotometric data were fitted with the program HypSpec.[2]

2. Characterizations of compounds

2.1) NMR spectra

*2.1.1) NMR spectra of compound **3***

FAN 415, $CDCl_3$, 400 MHz

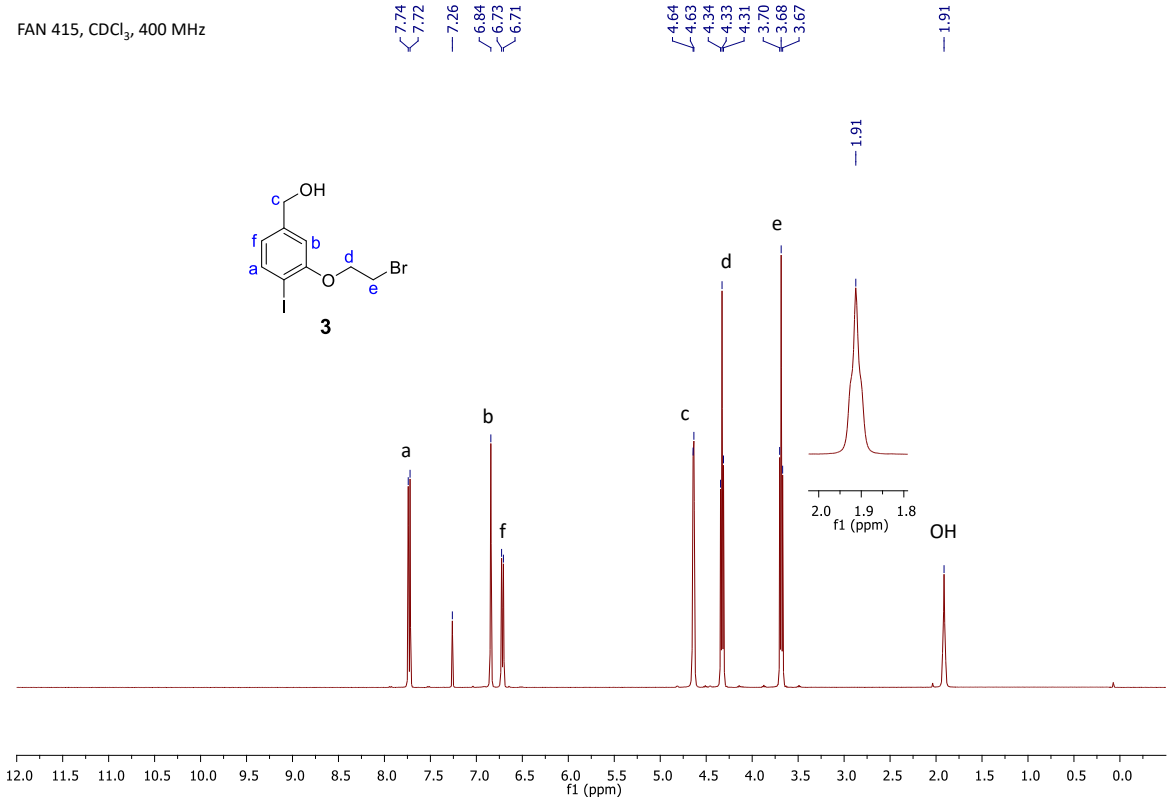

FAN 415, $CDCl_3$, 100 MHz

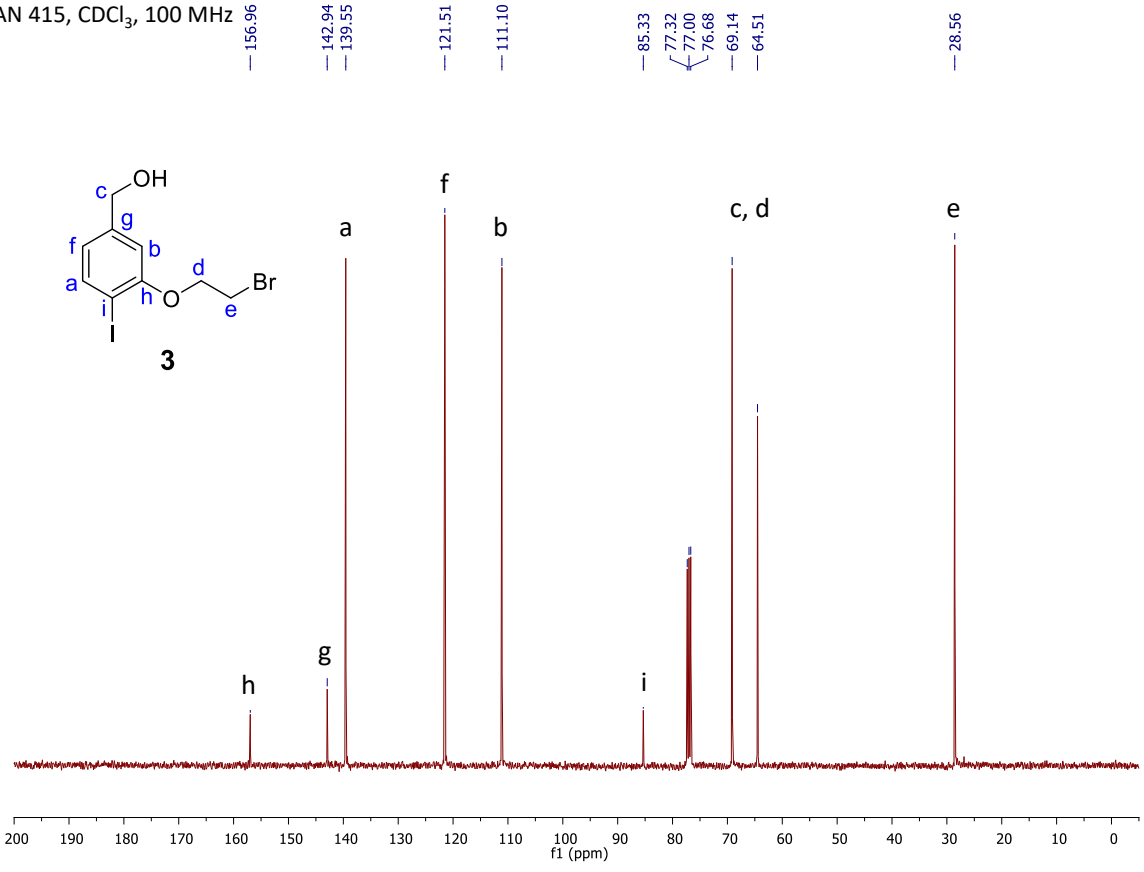

*2.1.2) NMR spectra of compound **4***

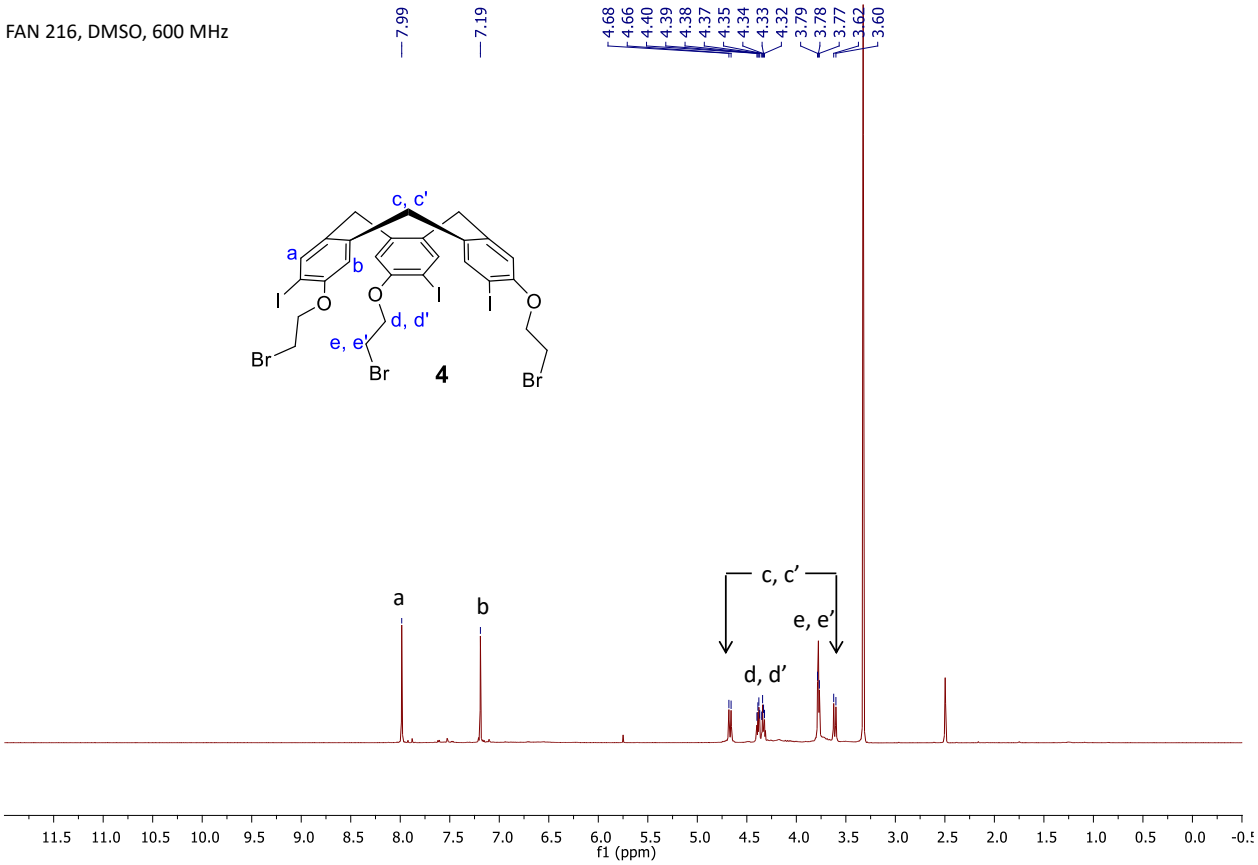

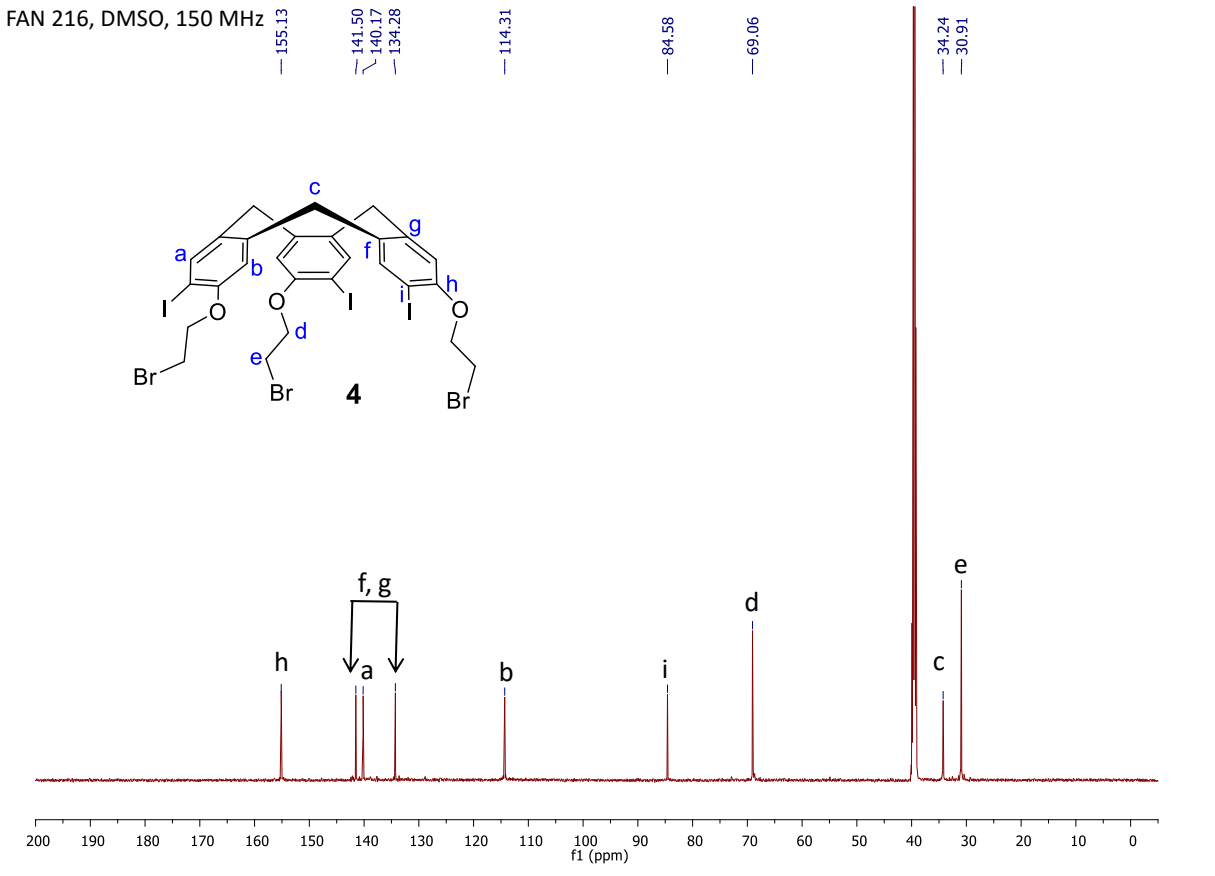

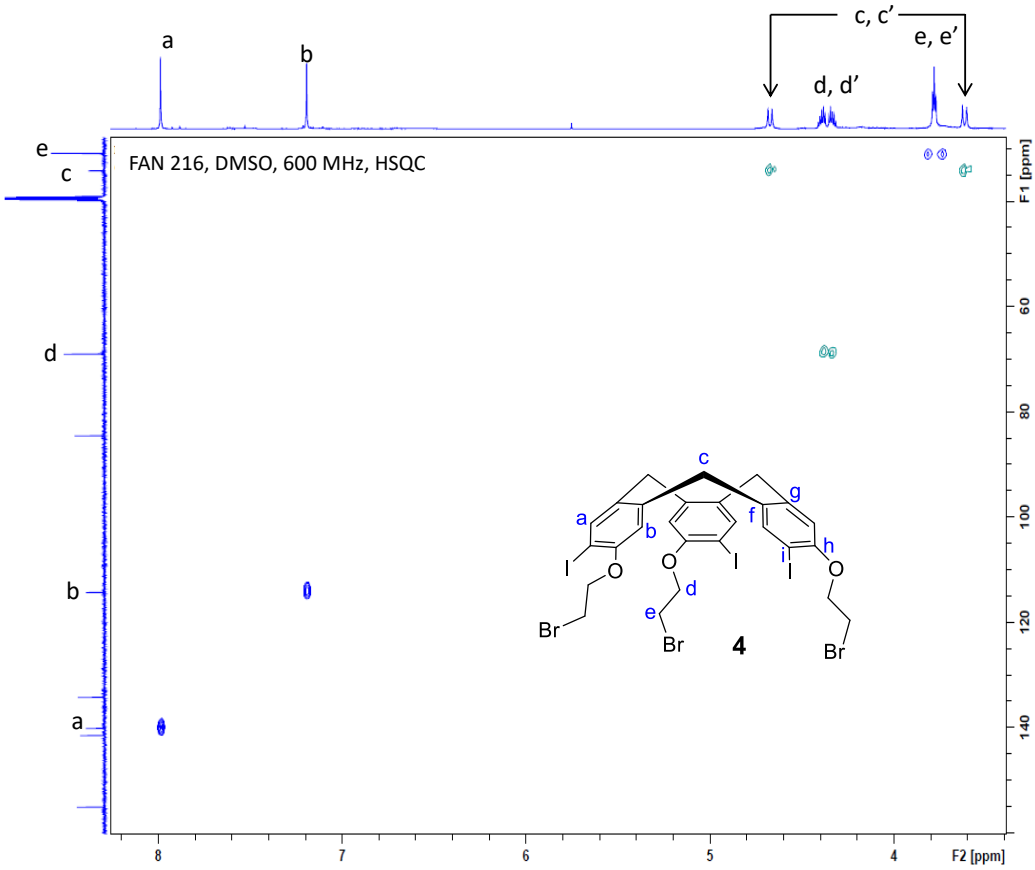
a
b
c, c'
e, e'
d, d'
e
c
FAN 216, DMSO, 600 MHz, HSQC
d
b
a
F1 [ppm]
F2 [ppm]
4

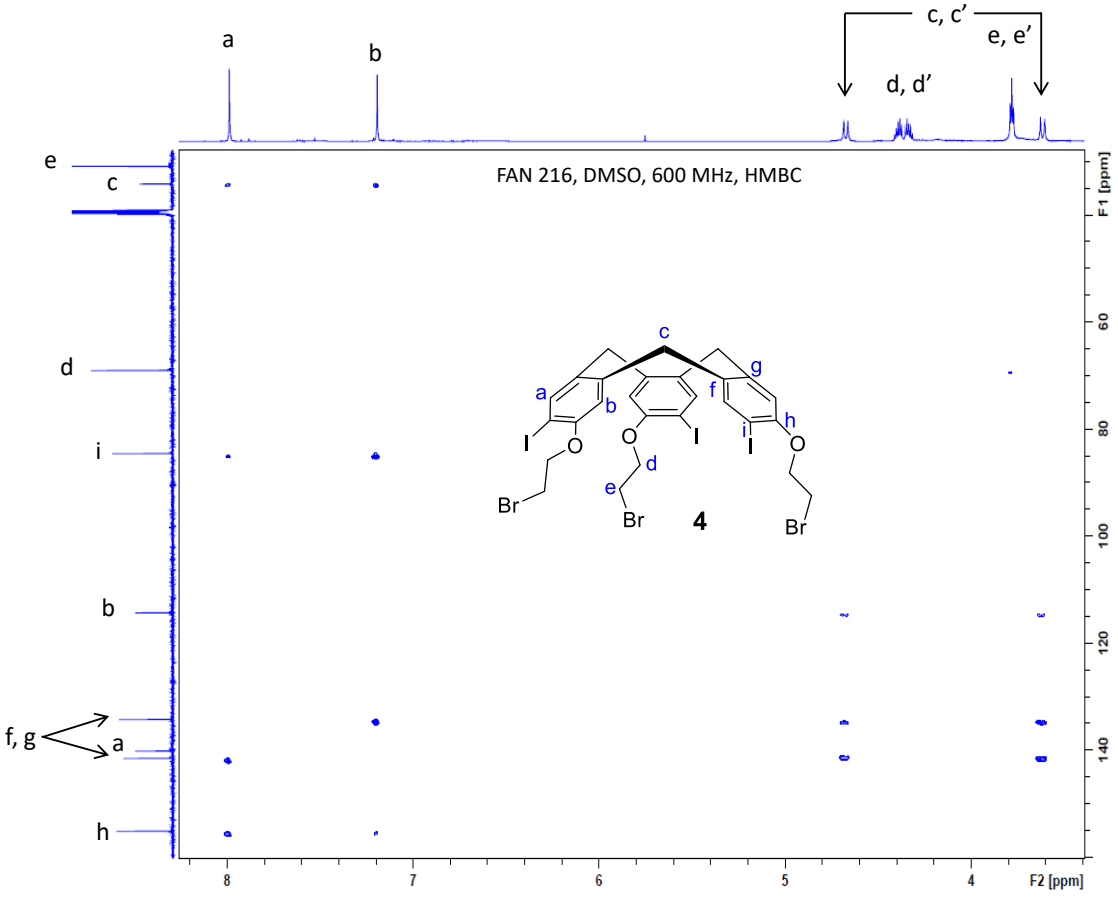
a
b
c, c'
e, e'
d, d'
e
c
FAN 216, DMSO, 600 MHz, HMBC
d
i
b
f, g
a
h
F1 [ppm]
F2 [ppm]
4

*2.1.3) NMR spectra of compound **5***

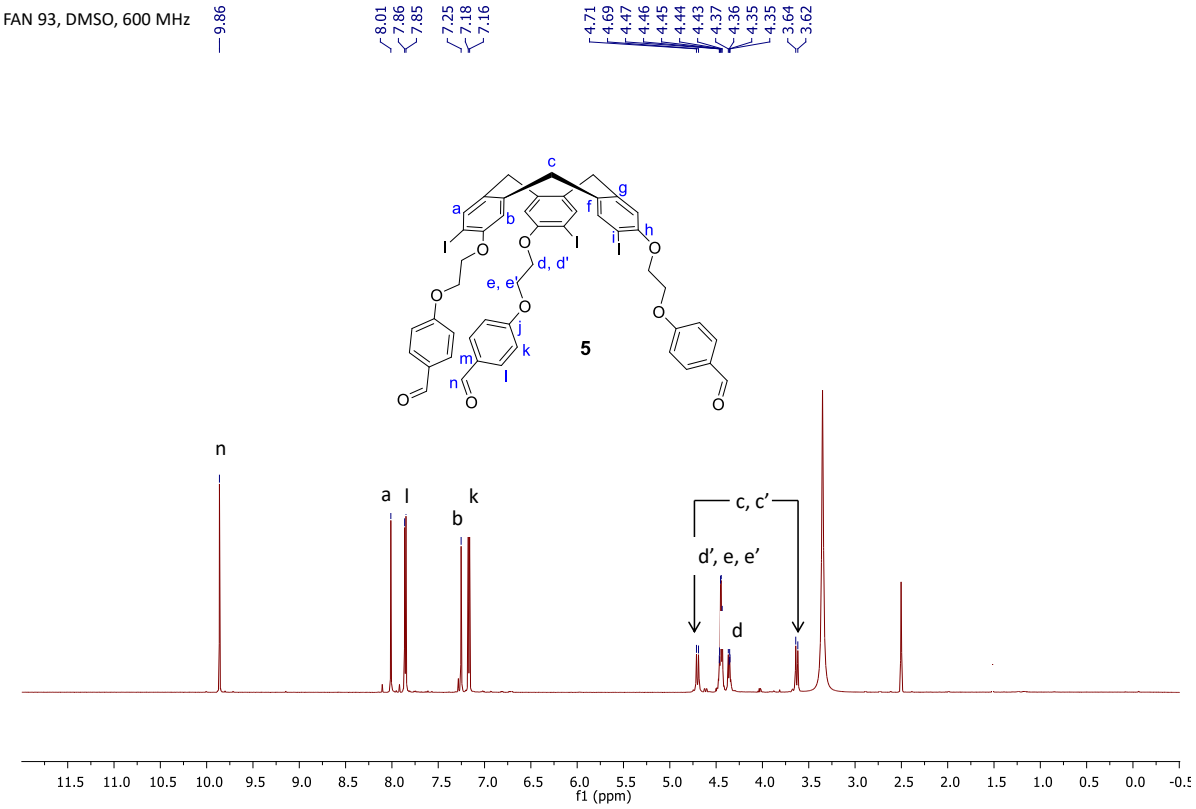

FAN 93, DMSO, 150 MHz

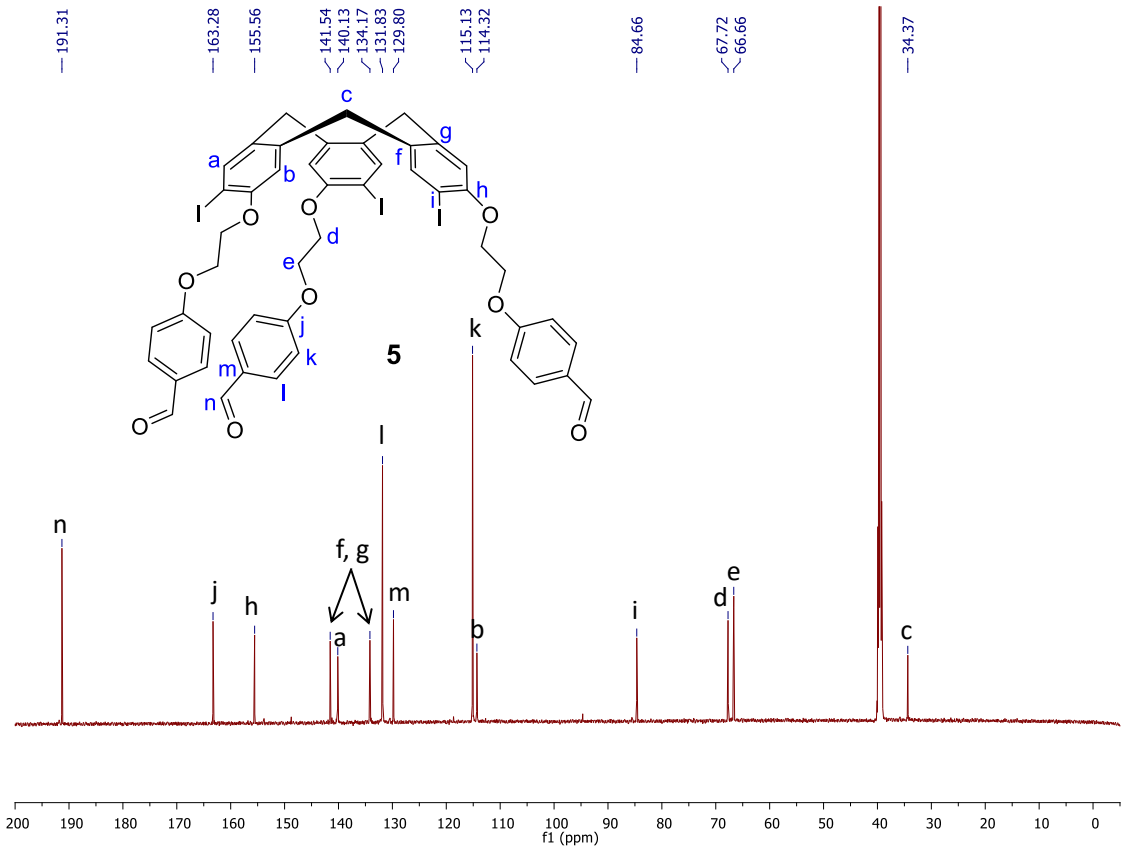

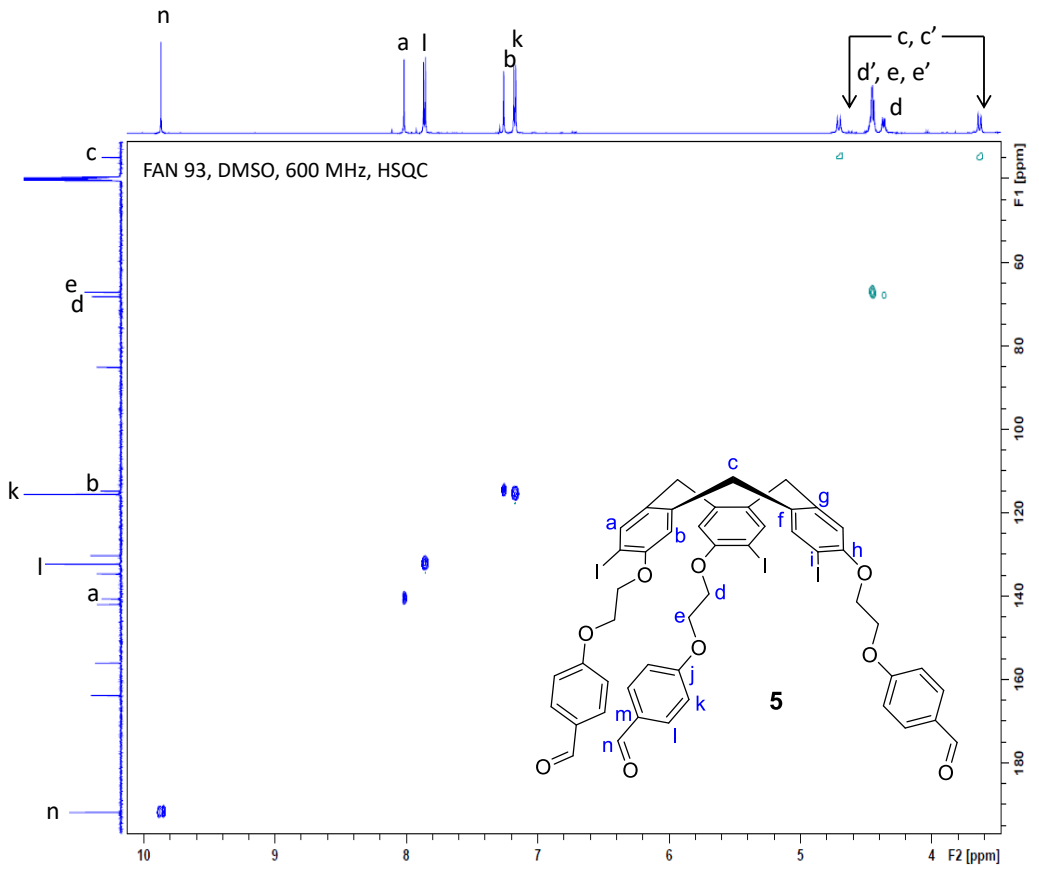
n
a l
k
b
c, c'
d', e, e'
d
FAN 93, DMSO, 600 MHz, HSQC
F1 [ppm]
F2 [ppm]
5

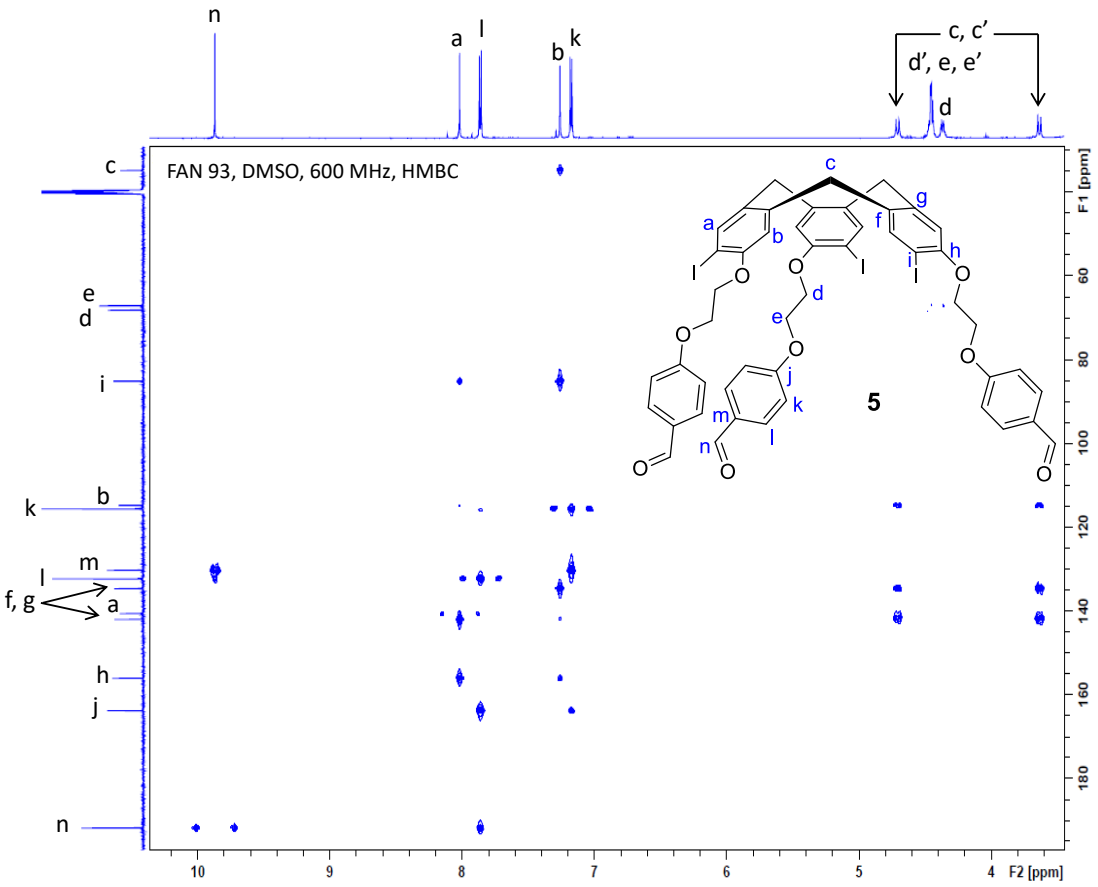
n
a l
b k
c, c'
d', e, e'
d
FAN 93, DMSO, 600 MHz, HMBC
F1 [ppm]
F2 [ppm]
5

*2.1.4) NMR spectra of compound **6***

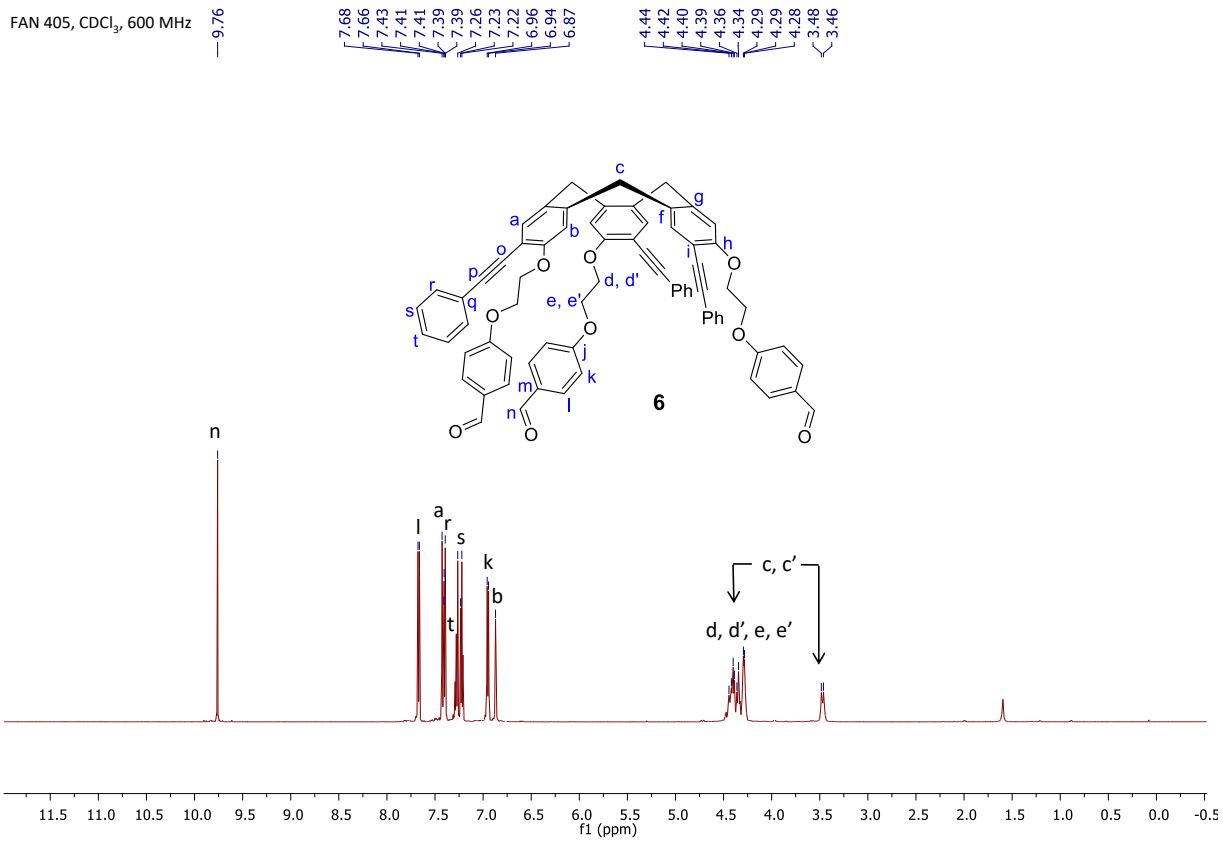

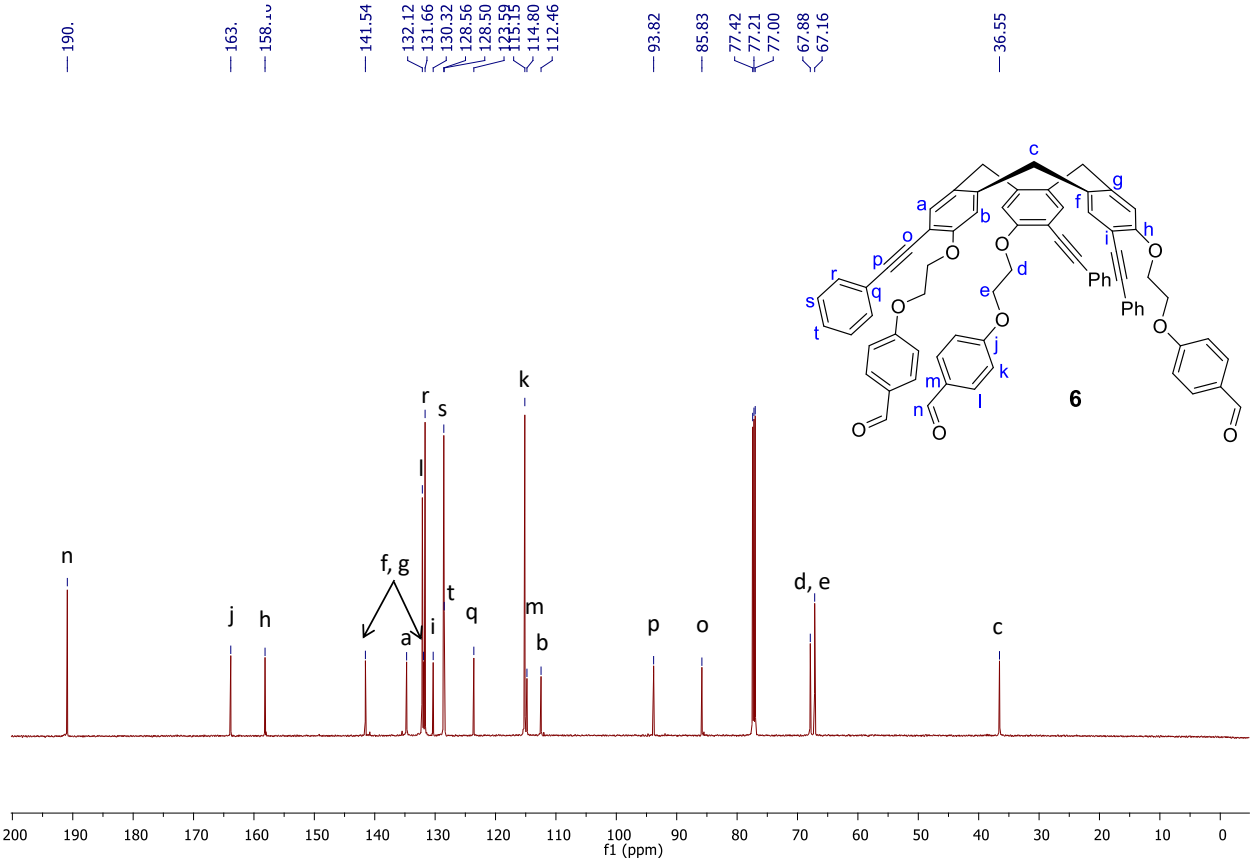

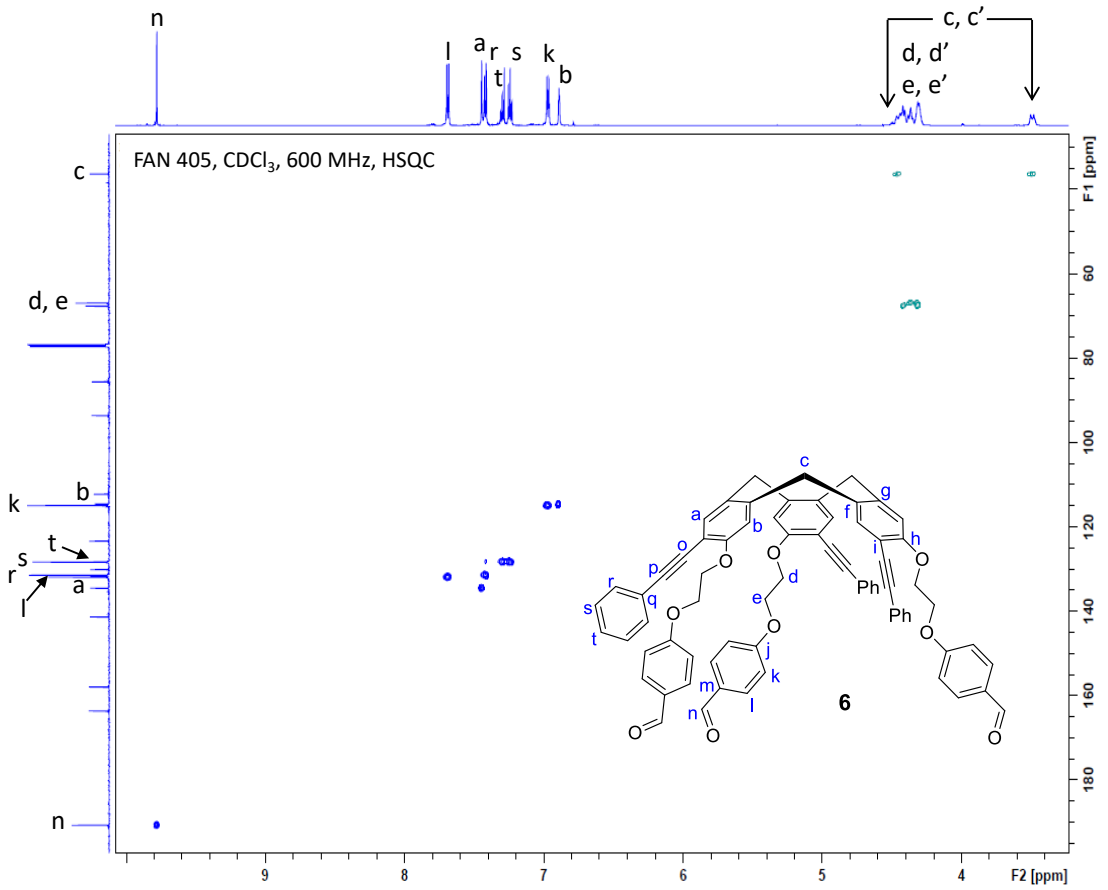
n
l
a
r
t
s
k
b
c, c'
d, d'
e, e'
FAN 405, CDCl3, 600 MHz, HSQC
c
d, e
k
b
t
s
r
a
l
n
6
F1 [ppm]
F2 [ppm]

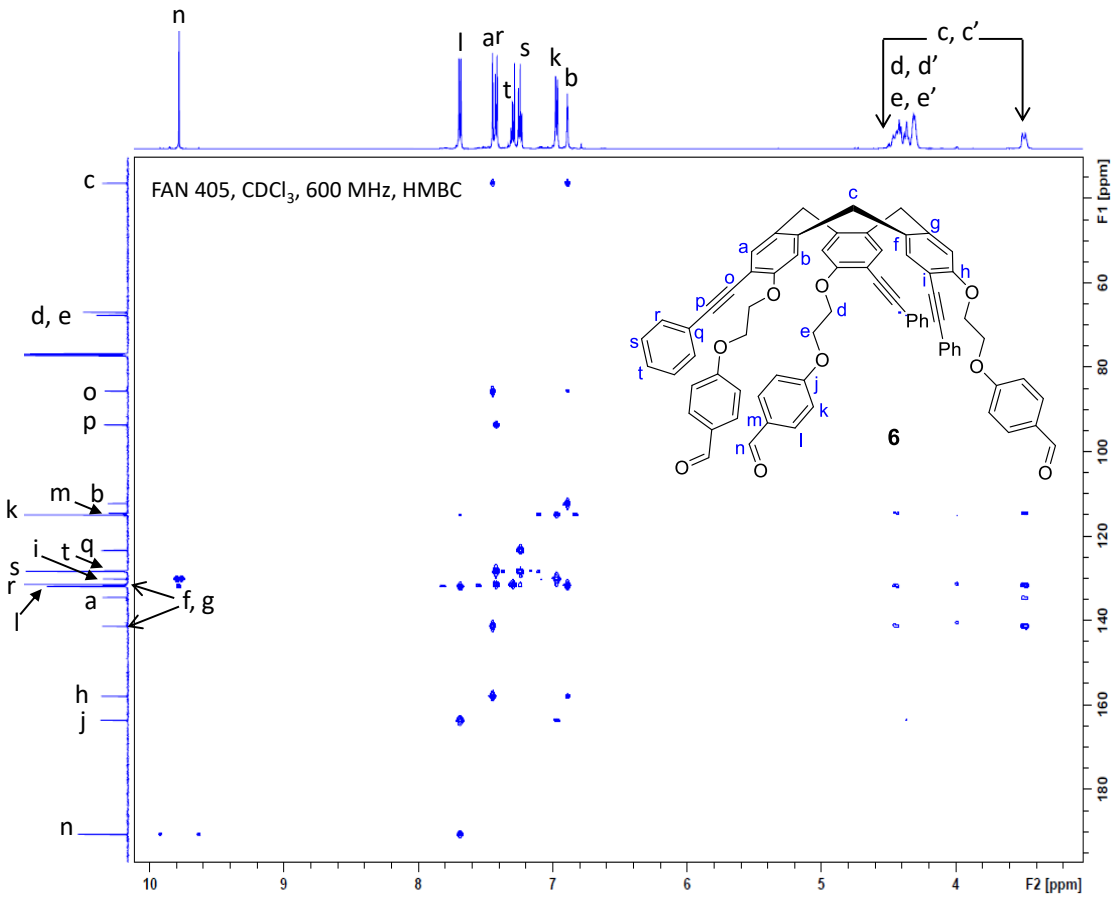
n
l
ar
t
s
k
b
c, c'
d, d'
e, e'
FAN 405, CDCl3, 600 MHz, HMBC
c
d, e
o
p
k
m
b
i
t
q
s
r
a
l
f, g
h
j
n
6
F1 [ppm]
F2 [ppm]

*2.1.5) NMR spectra of hemicryptophane **1***

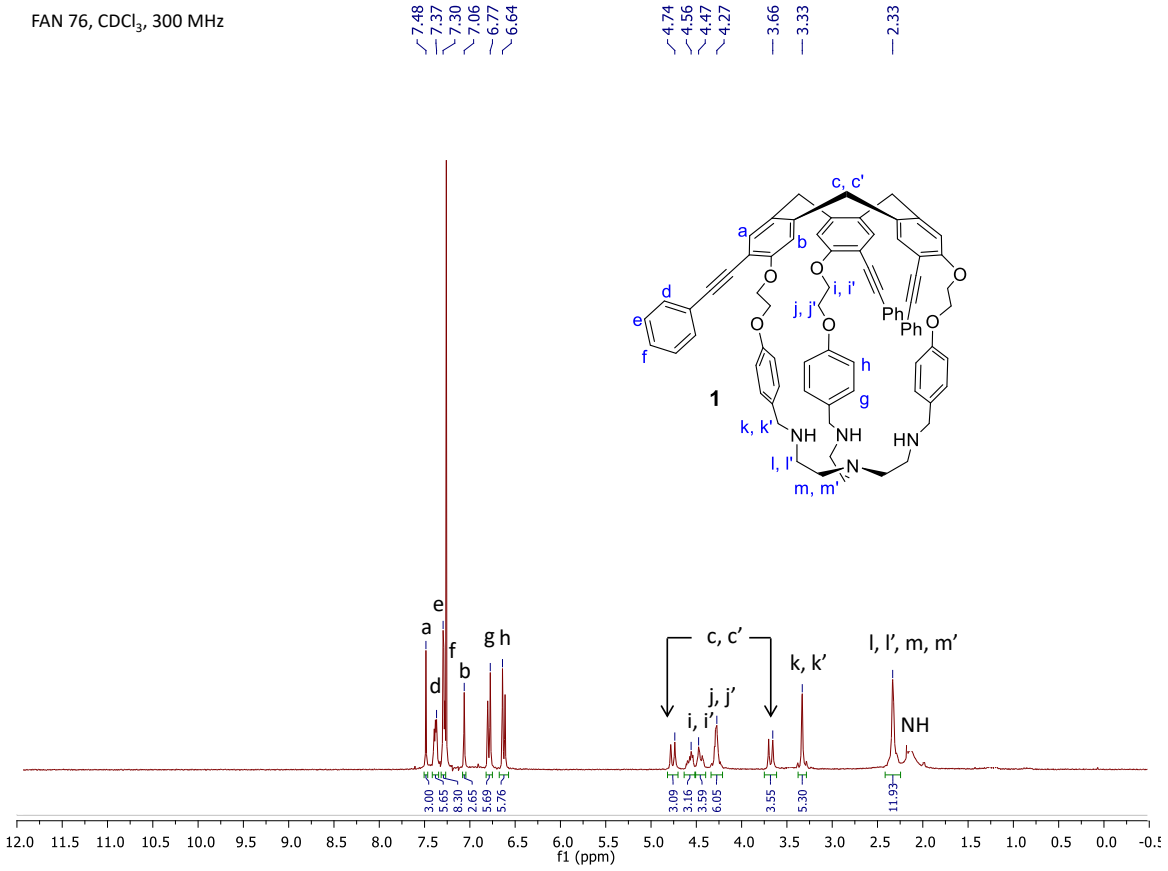

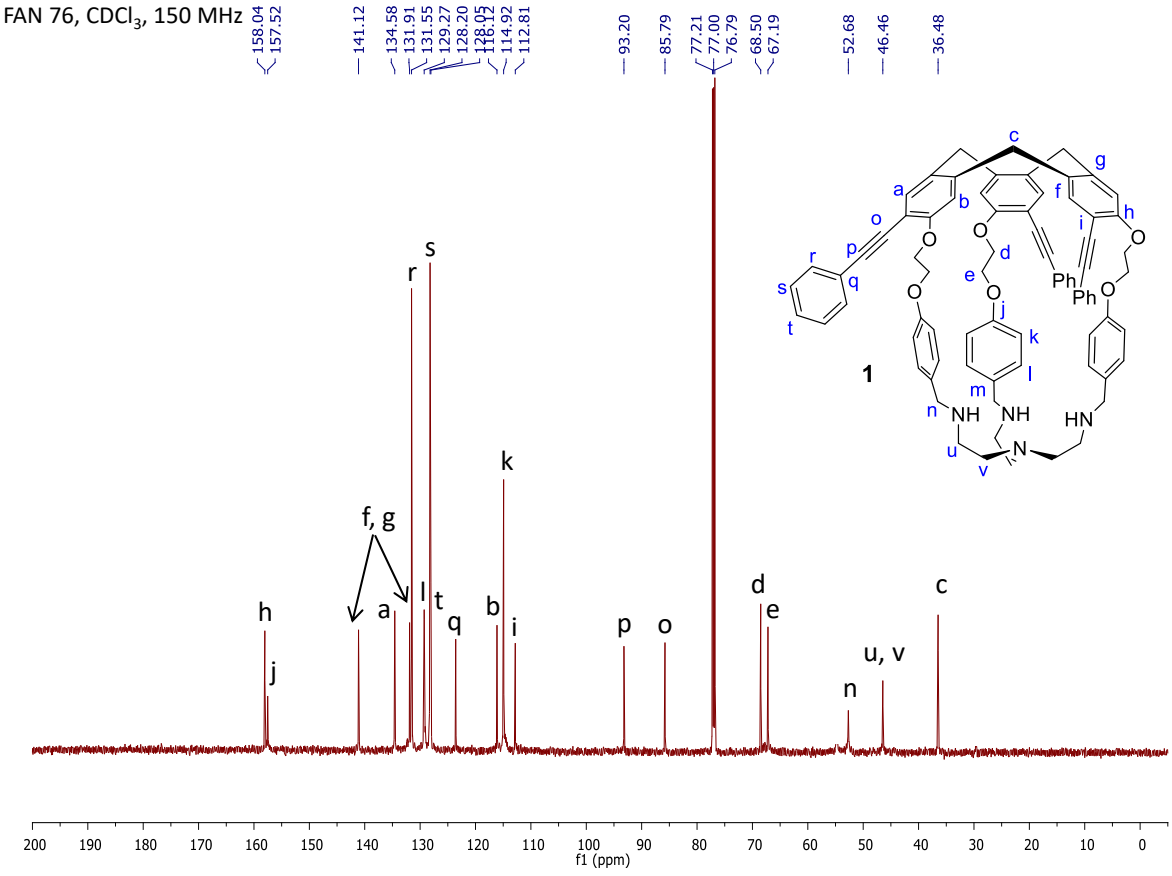

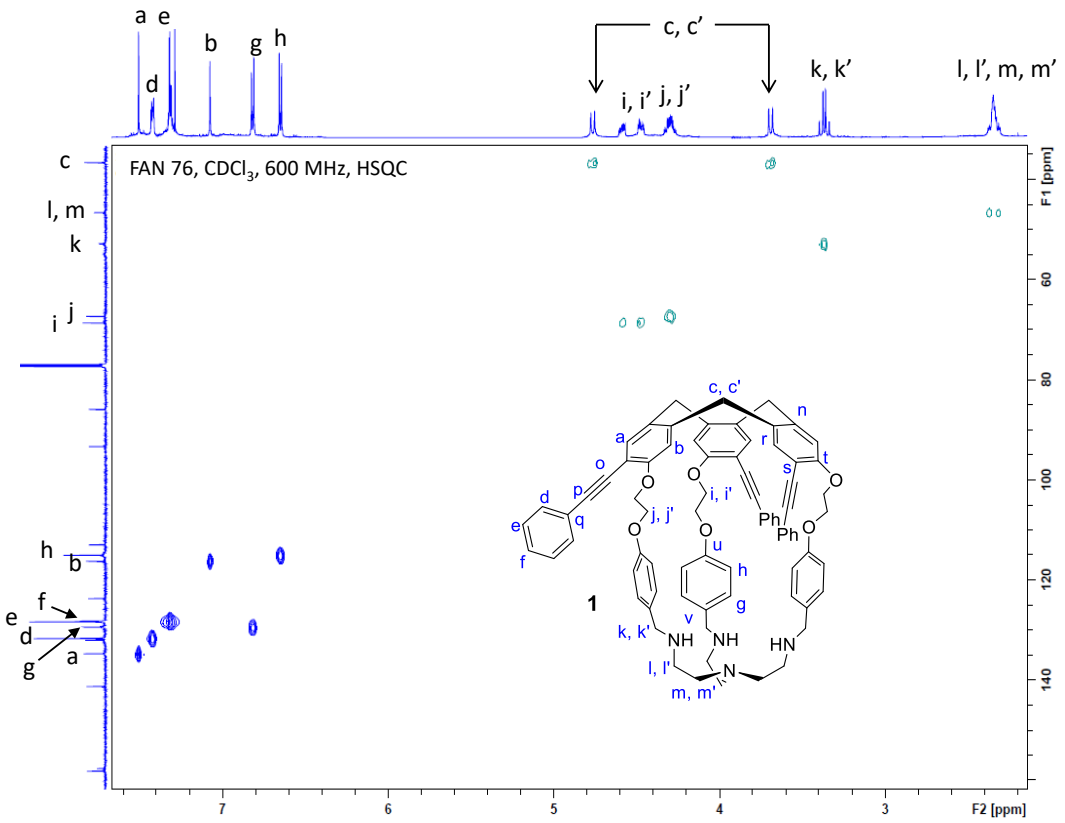
a e
b g h
d
c, c'
i, i' j, j'
k, k'
l, l', m, m'
FAN 76, CDCl3, 600 MHz, HSQC
c
l, m
k
i j
h
b
f
e
d
g
a
F1 [ppm]
F2 [ppm]
1

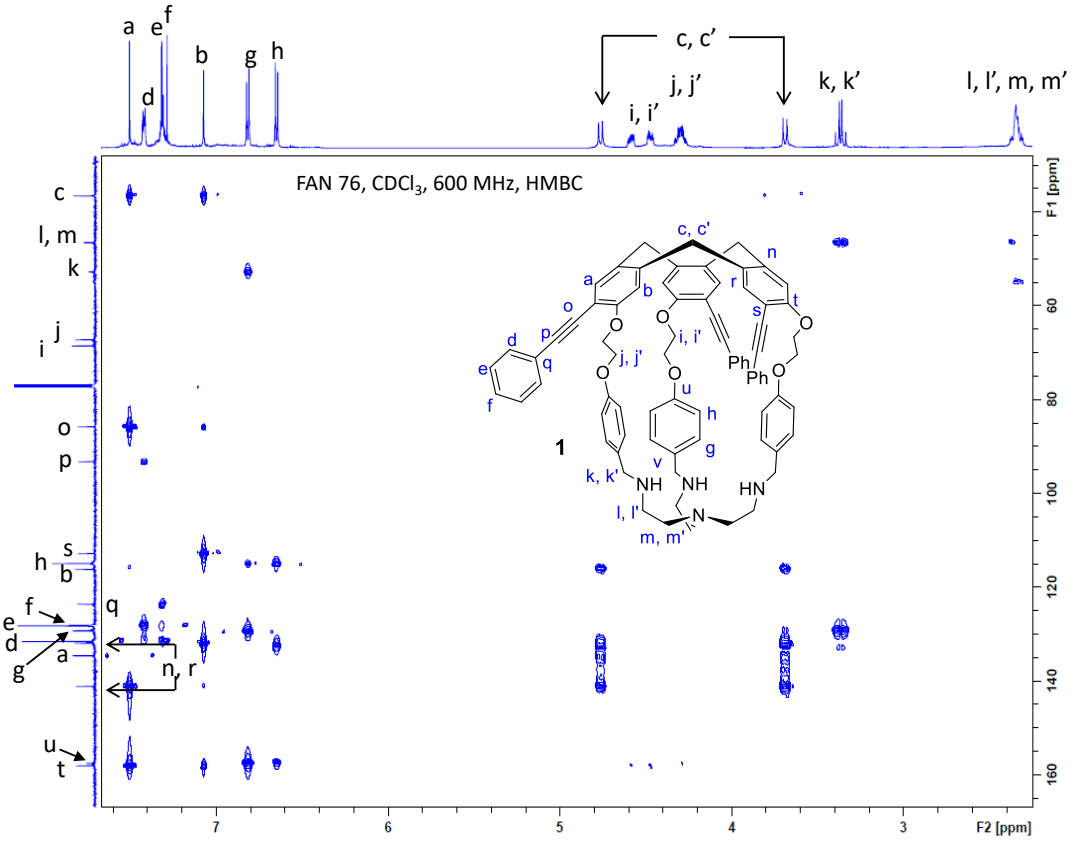
a e f
b g h
d
c, c'
i, i'
j, j'
k, k'
l, l', m, m'
FAN 76, CDCl3, 600 MHz, HMBC
c
l, m
k
i j
o
p
h s
b
f
q
e
d
a
g
n, r
u
t
F1 [ppm]
F2 [ppm]
1

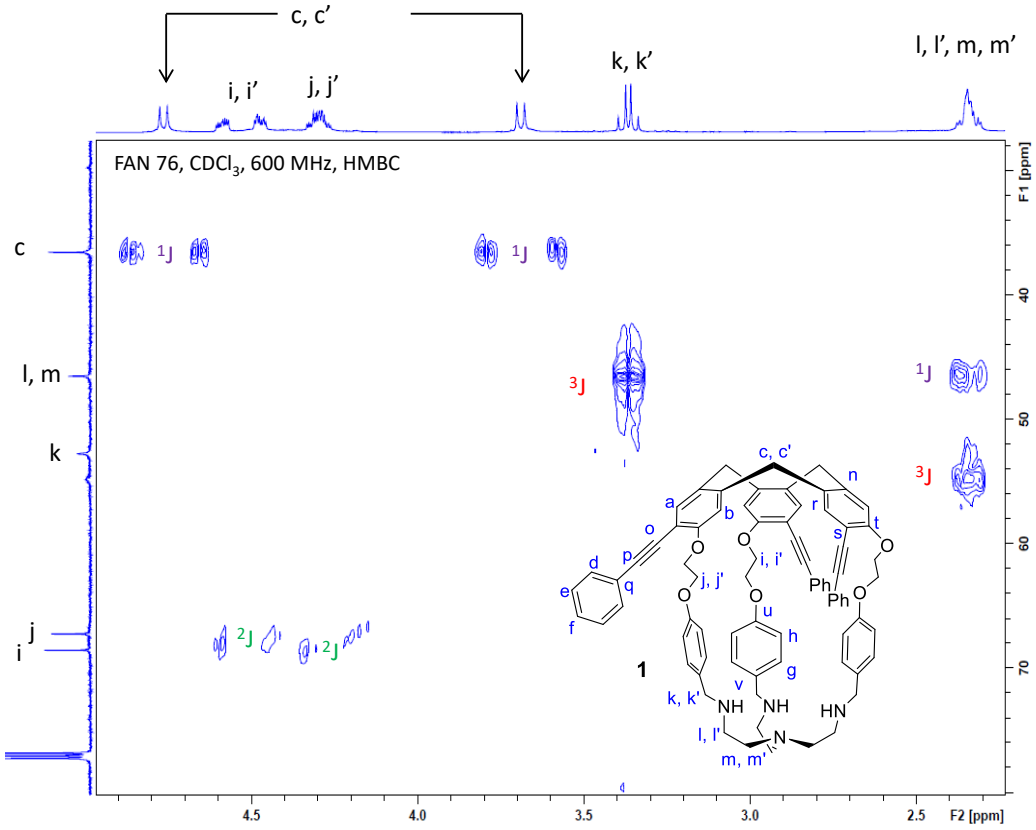
c, c'
i, i'
j, j'
k, k'
l, l', m, m'
FAN 76, CDCl3, 600 MHz, HMBC
c
l, m
k
j
i
1J
2J
3J
F1 [ppm]
F2 [ppm]
1

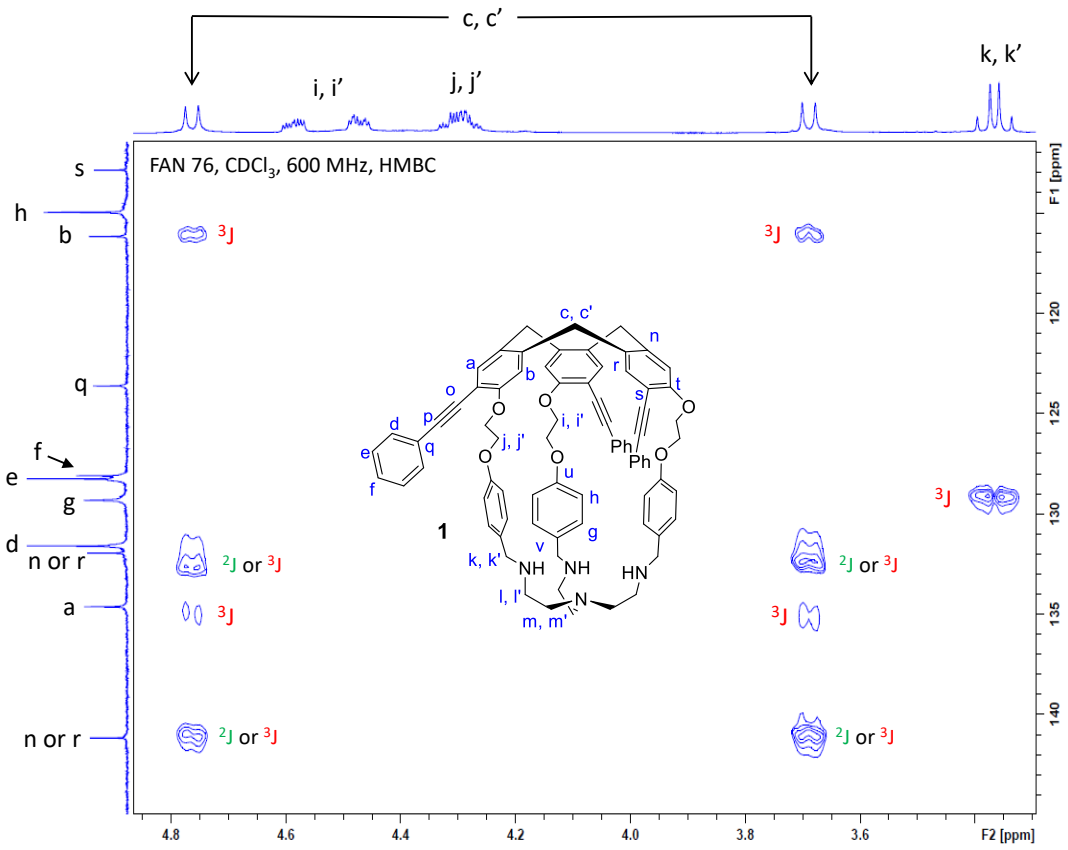
c, c'
i, i'
j, j'
k, k'
FAN 76, CDCl3, 600 MHz, HMBC
s
h
b
q
f
e
g
d
n or r
a
n or r
3J
2J or 3J
F1 [ppm]
F2 [ppm]
1

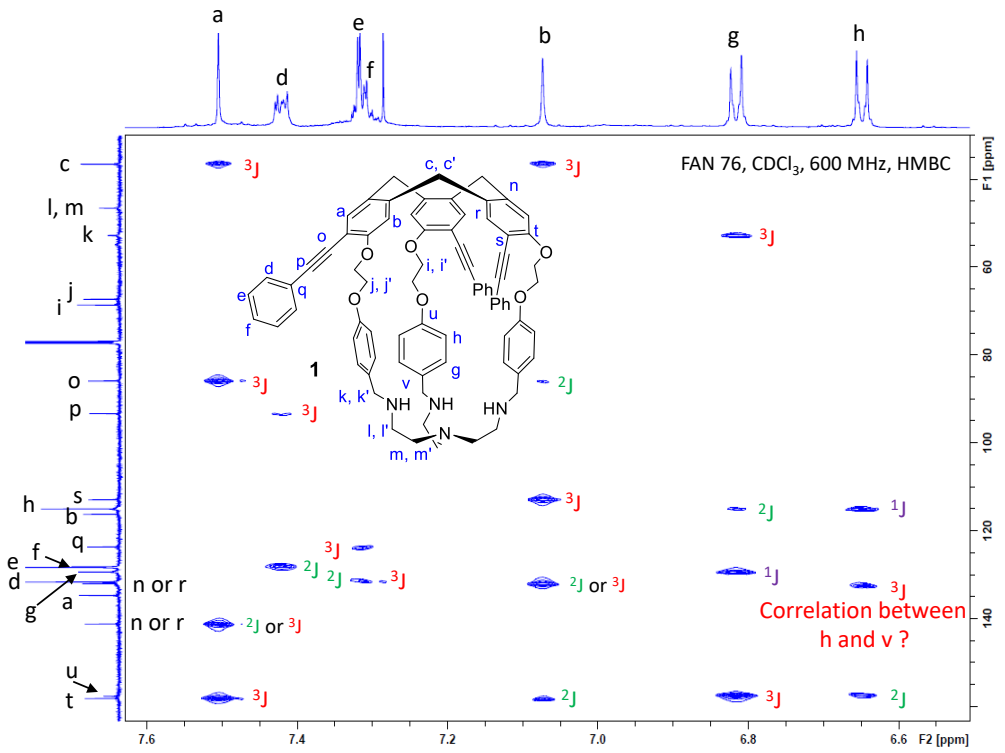

The HMBC spectrum shows a correlation spot that can be attributed to carbon v. However, we were unable to confirm this by JMOD experiment. This result indicates that the quaternary carbon v is probably confused with another carbon signal, d, n or r.

2.2) IR spectra

*2.2.1) IR spectrum of compound **3***

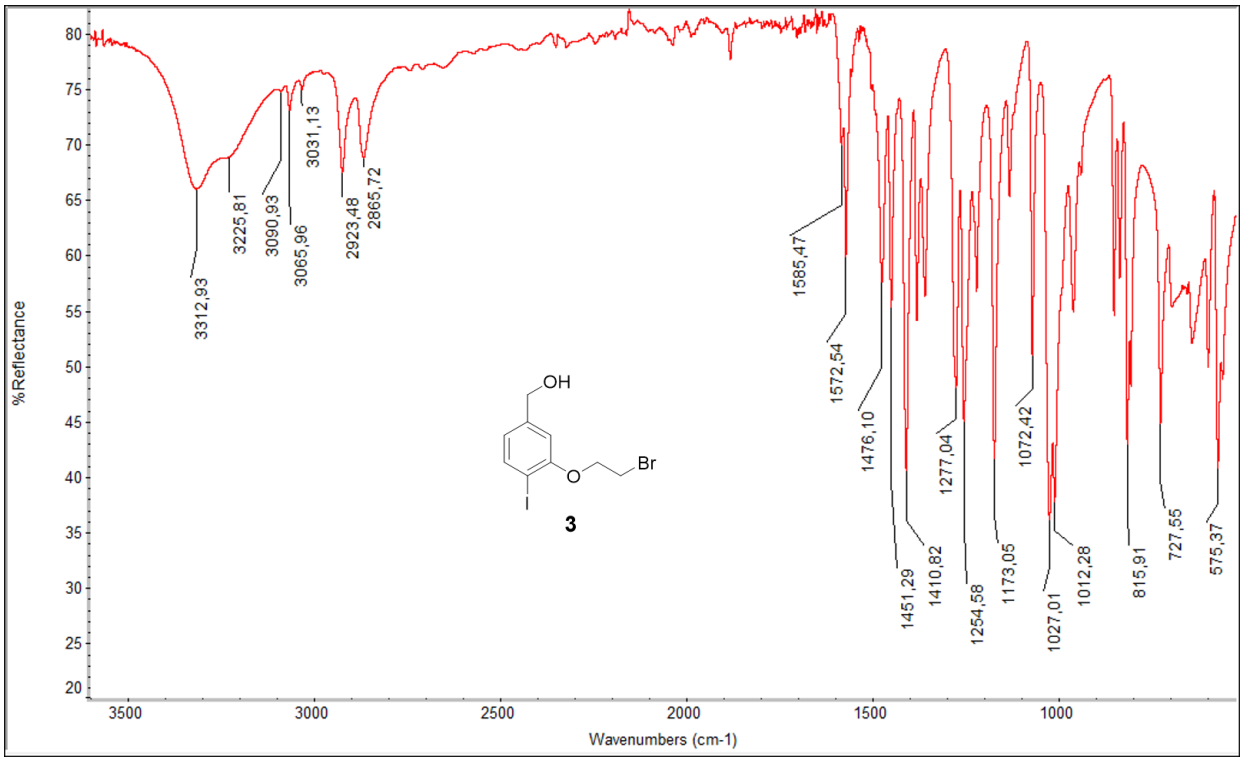

*2.2.2) IR spectrum of compound **4***

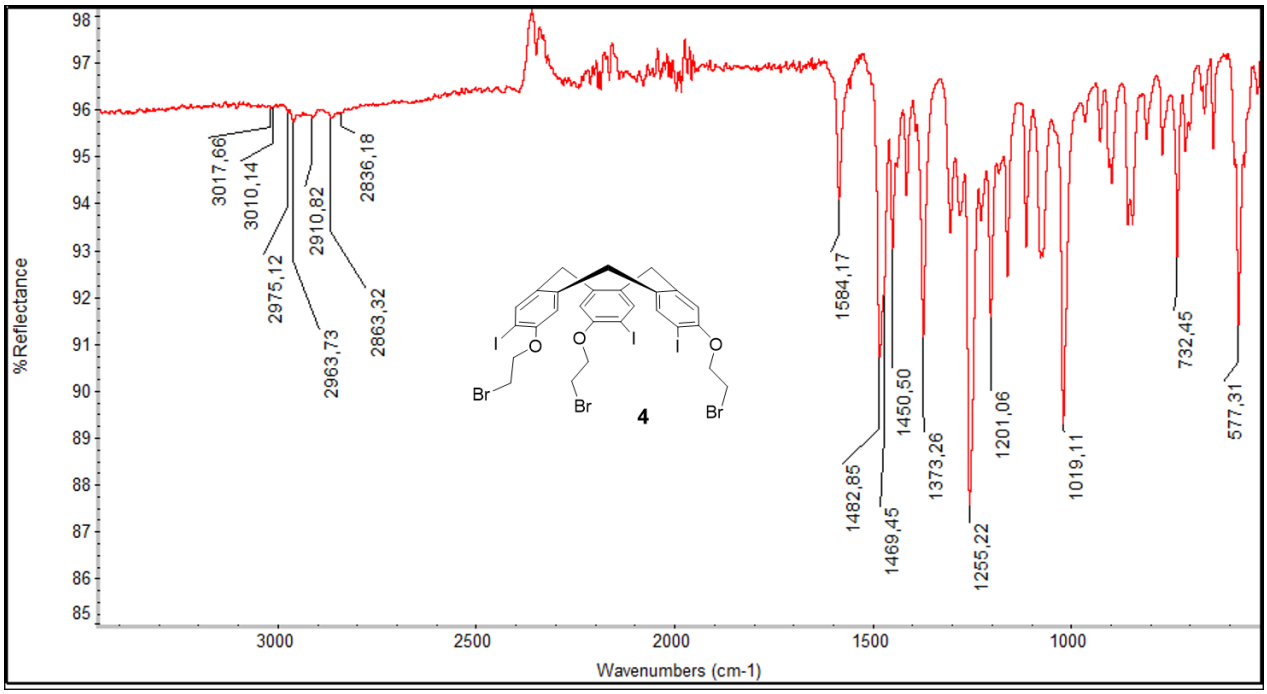

*2.2.3) IR spectrum of compound **5***

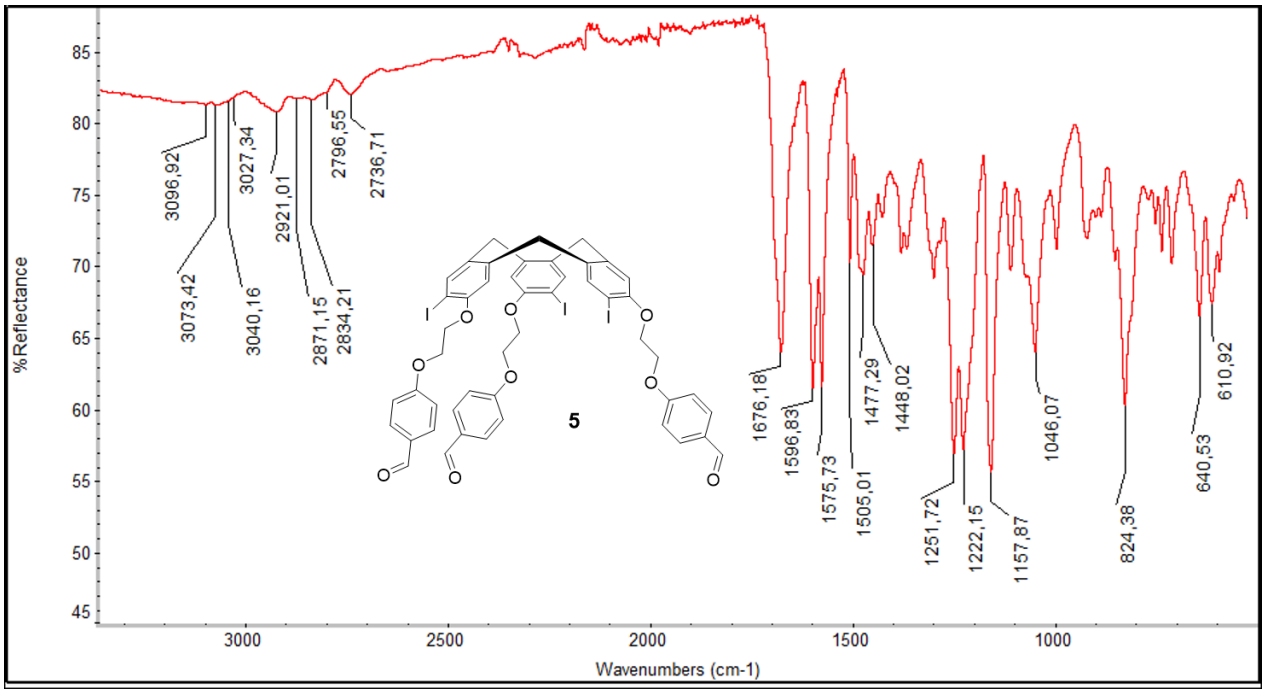

*2.2.4) IR spectrum of compound **6***

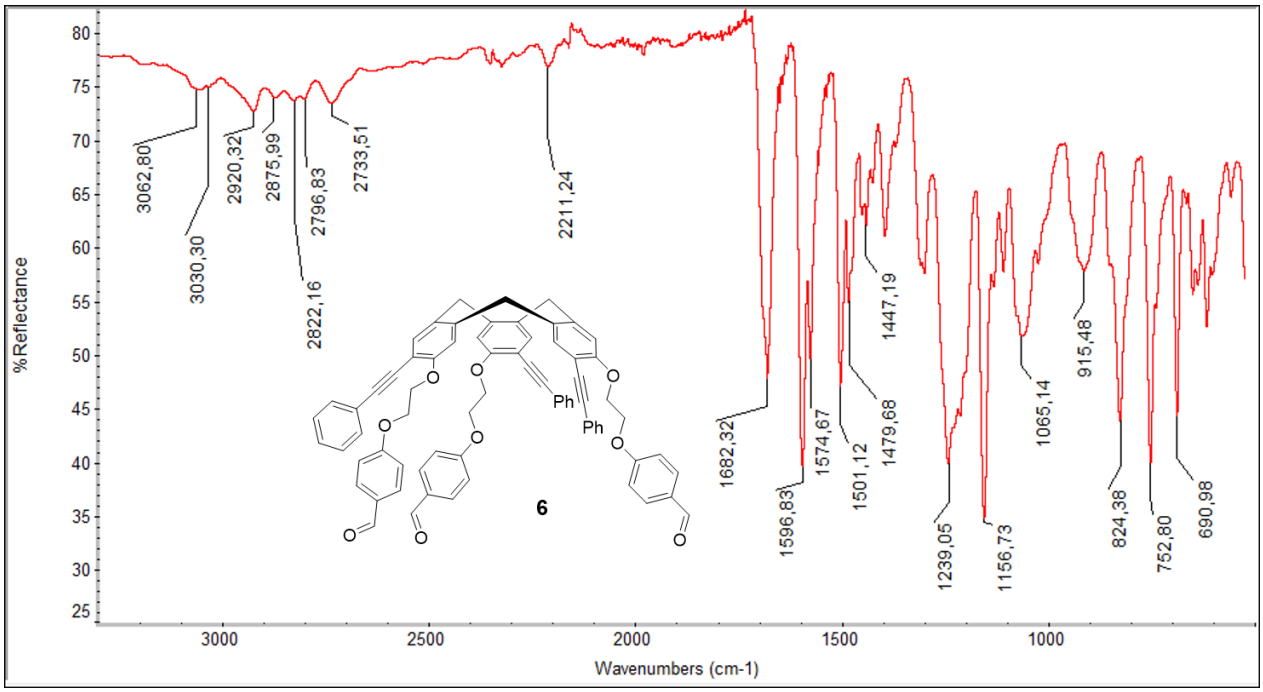

*2.2.5) IR spectrum of compound **1***

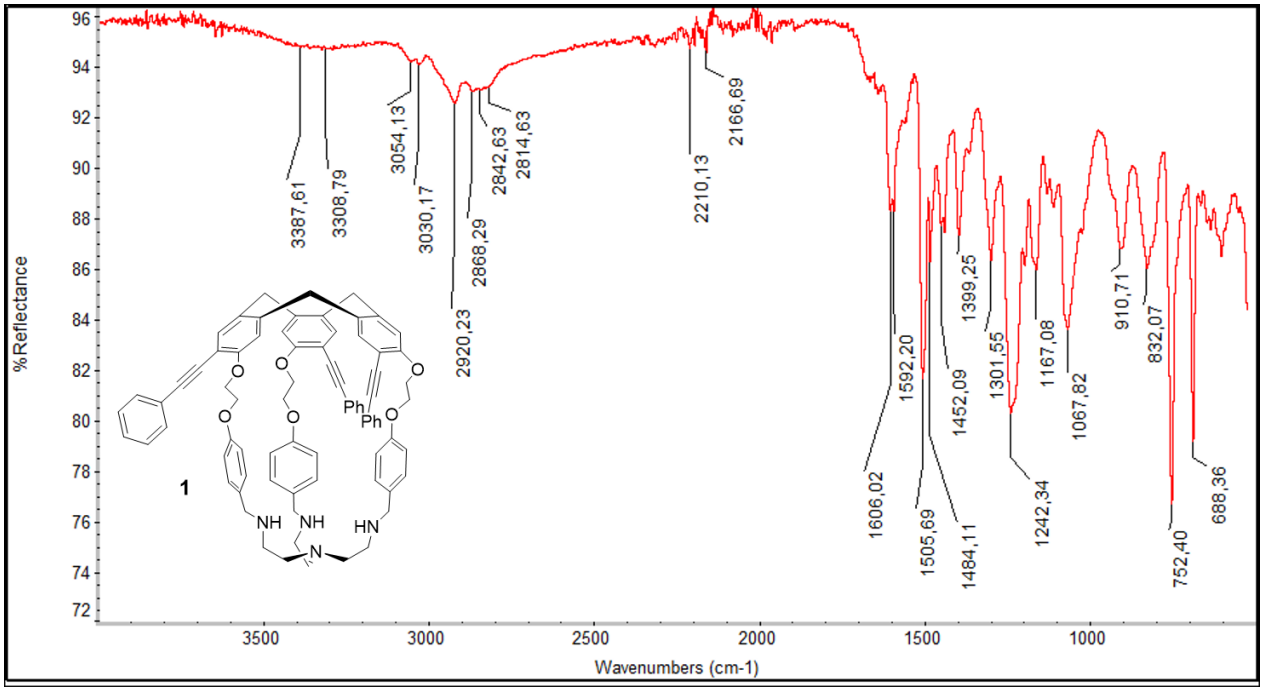

2.3) HRMS spectra

*2.3.1) HRMS of compound **3***

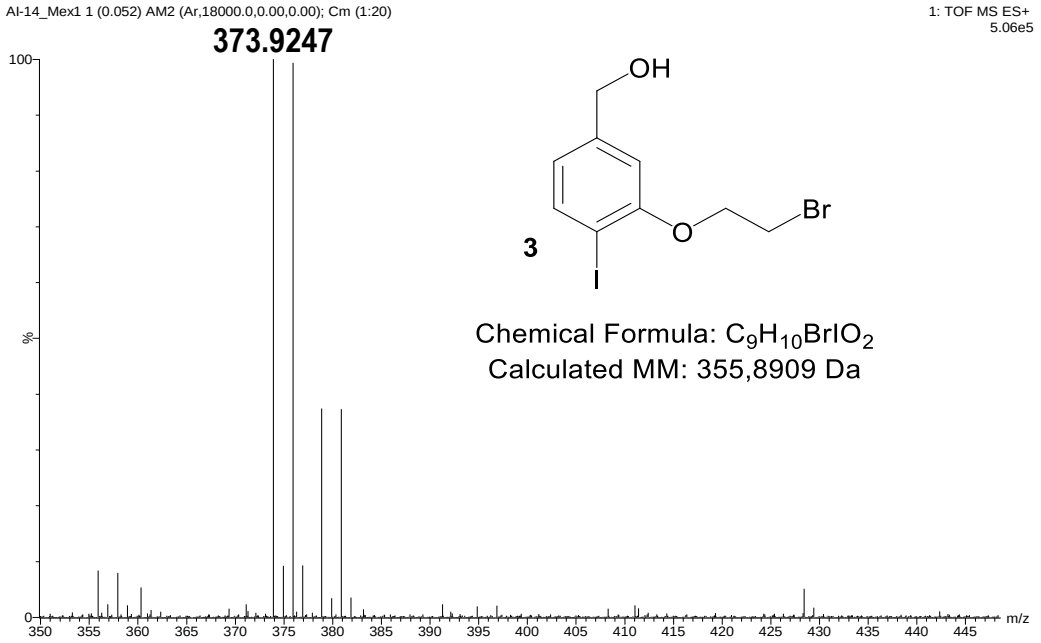

High Resolution Mass spectra of compound **3** (ESI, positive mode). The $[M+NH_4]^+$ targeted ion is detected at m/z 373.9247.

*2.3.2) HRMS of compound **4***

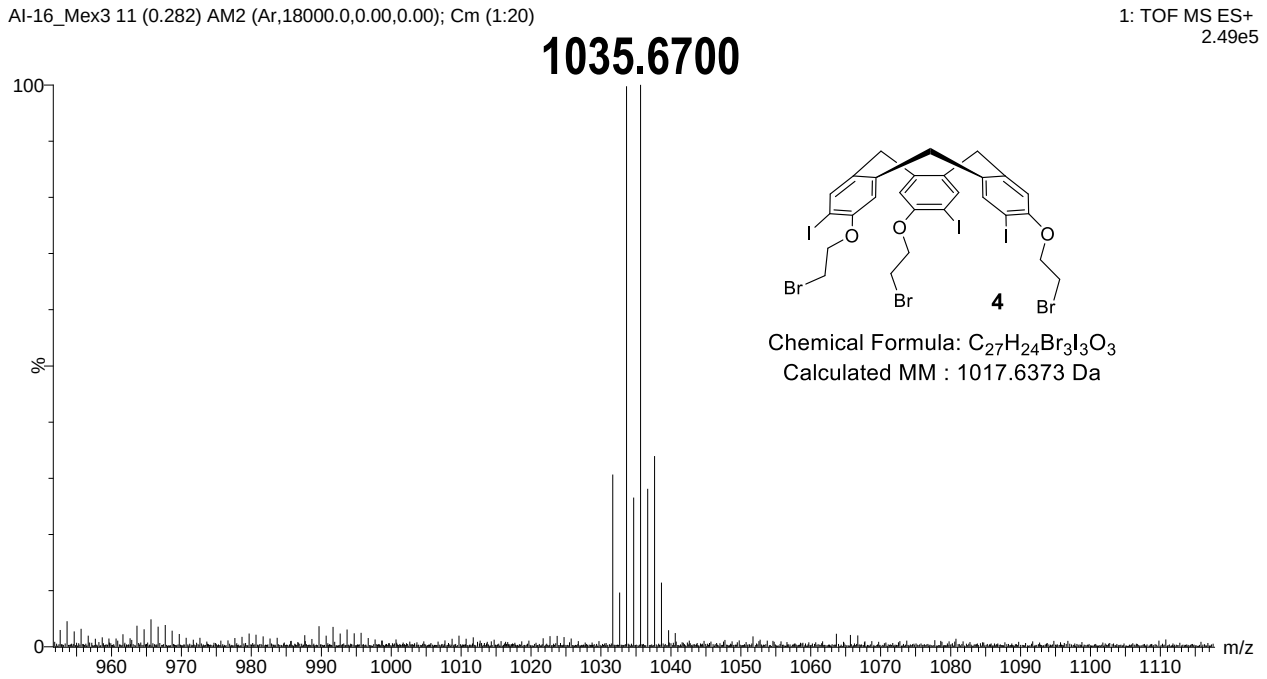

High Resolution Mass spectra of compound **4** (ESI, positive mode). The $[M+NH_4]^+$ targeted ion is detected at m/z 1035.6700.

*2.3.3) HRMS of compound **5***

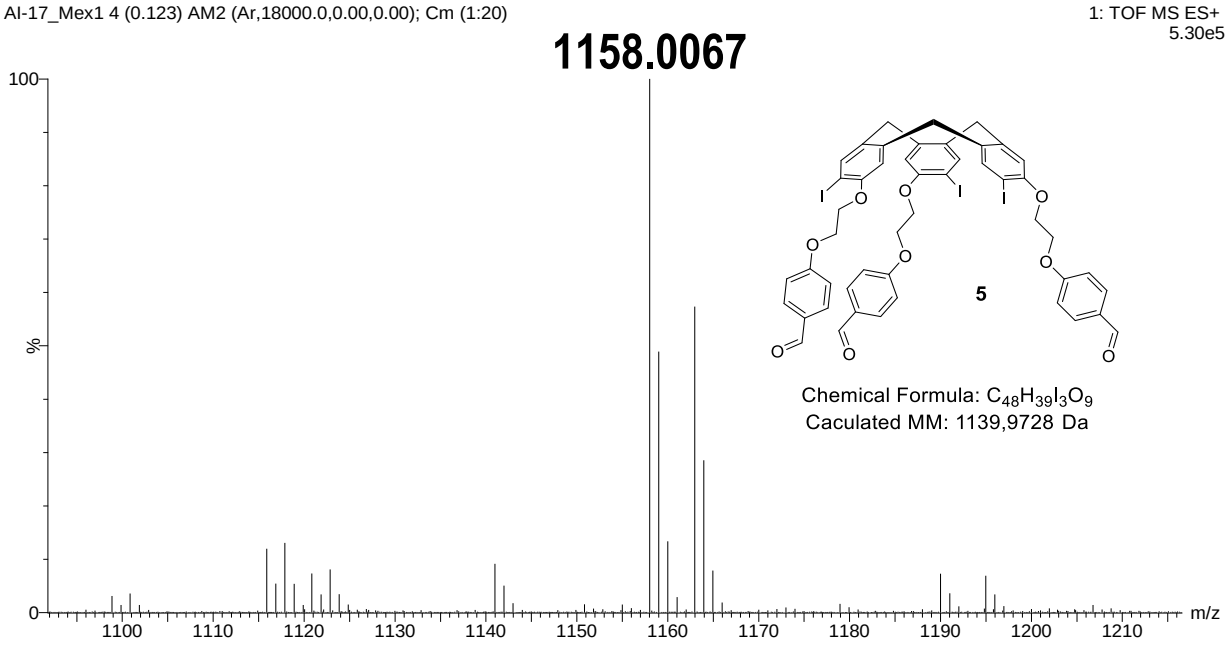

High Resolution Mass spectra of compound **5** (ESI, positive mode). The $[M+NH_4]^+$ targeted ion is detected at m/z 1158.0067.

*2.3.4) HRMS of compound **6***

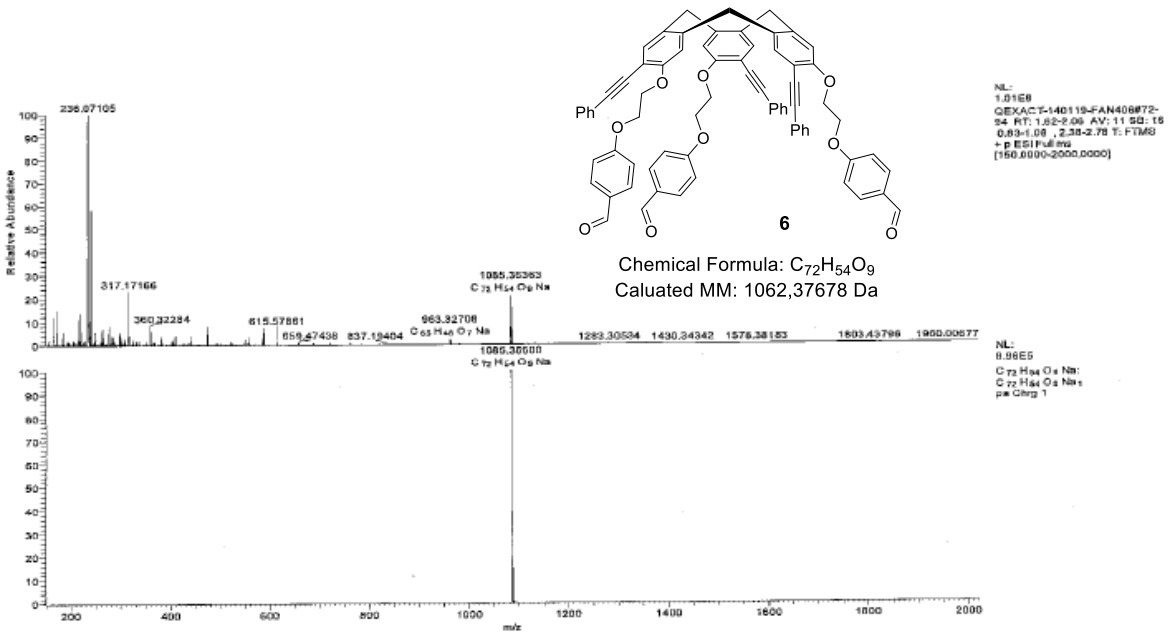

Calcul Haute Resolution HR en ESI mode + avec Orbitrap Q exactive plus de Thermoscientific

Elemental composition search on mass 1085.36366

m/z= 1080.36366-1090.36366

m/z	Theo. Mass	Delta (ppm)	RDB equiv.	Composition
1085.36366	1085.36600	-2.16	45.5	C72 H54 O9 Na

High Resolution Mass spectra of compound **6** (ESI, positive mode). The $[M+H]^+$ targeted ion is detected at m/z 1085.36366.

*2.3.5) HRMS of hemicryptophane **1***

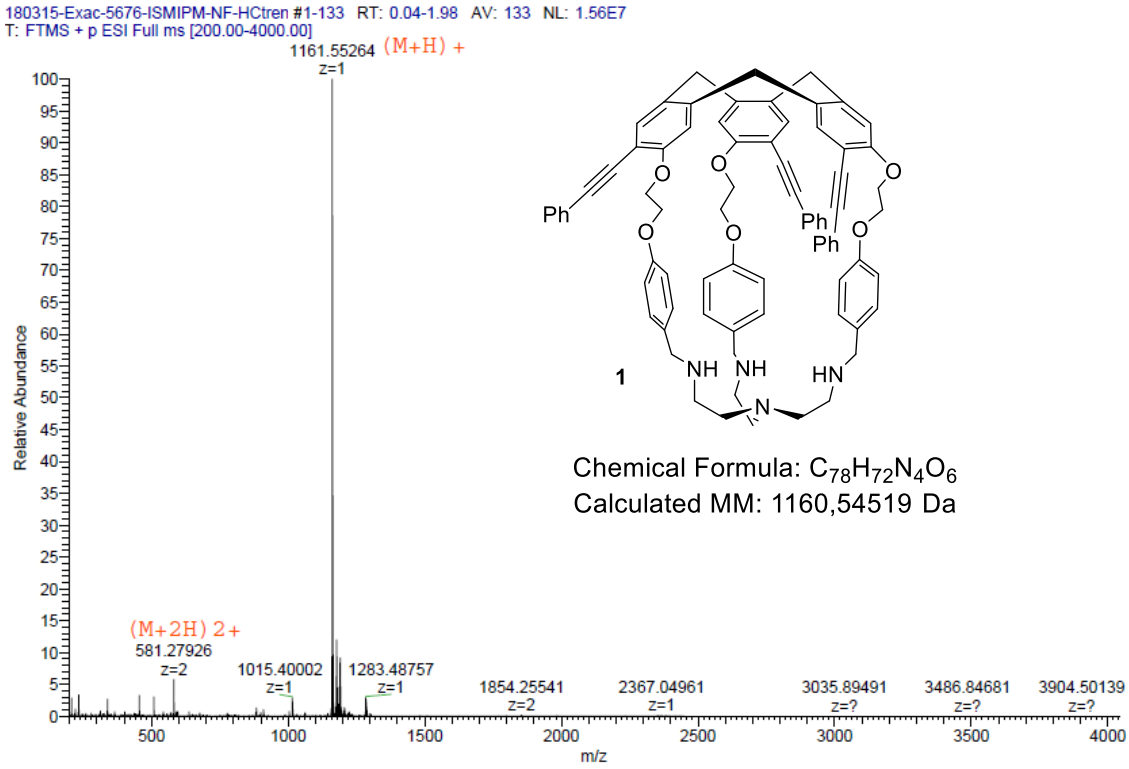

High Resolution Mass spectra of compound **2** (ESI, positive mode). The $[M+H]^+$ targeted ion is detected at m/z 1161.55264.

3. Fluorescence experiments

3.1) Spectroscopic characterisation

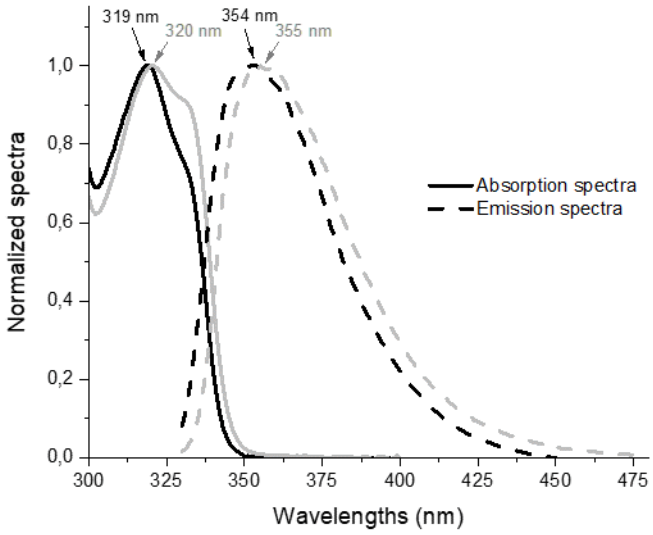

Fig. S1. Normalized absorption and emission spectra of the HC **1** in chloroform/methanol (98/2) (in black) and the analogous CTV in DMSO[1] (in grey).

3.2) Titration of acetylcholine

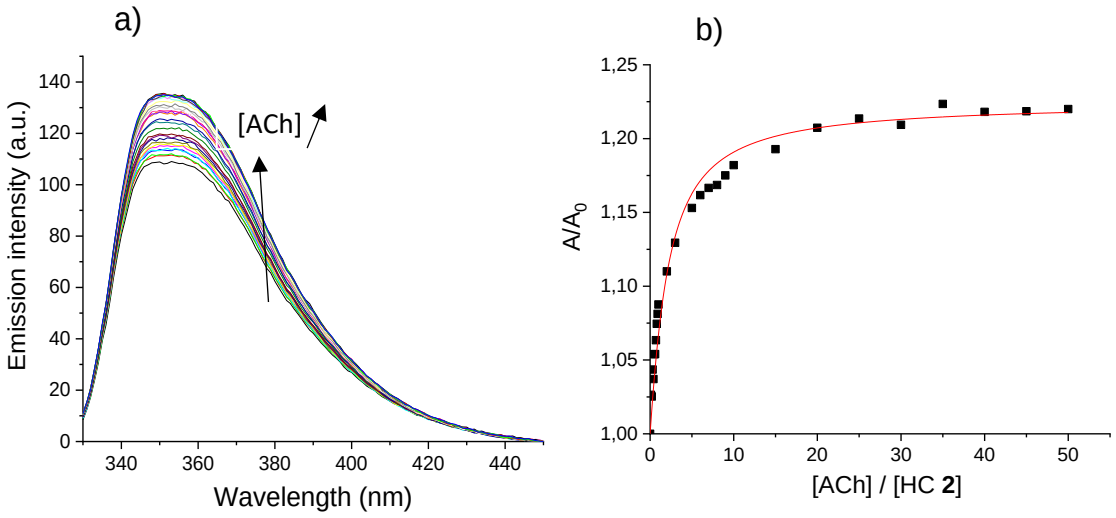

Fig. S2. a) Fluorescence emission enhancement of a 2.10^{-5}M hemicryptophane **1** solution upon addition of a solution of acetylcholine chloride (λ_{ex}=319 nm). b) Relative fluorescence area of **1** (10^{-5} M) with increasing amount of ACh (0 to 50 eq.). (-) acetylcholine fitted with a 1:1 binding model.

3.3) Binding constants determination using Hypspec®[2]

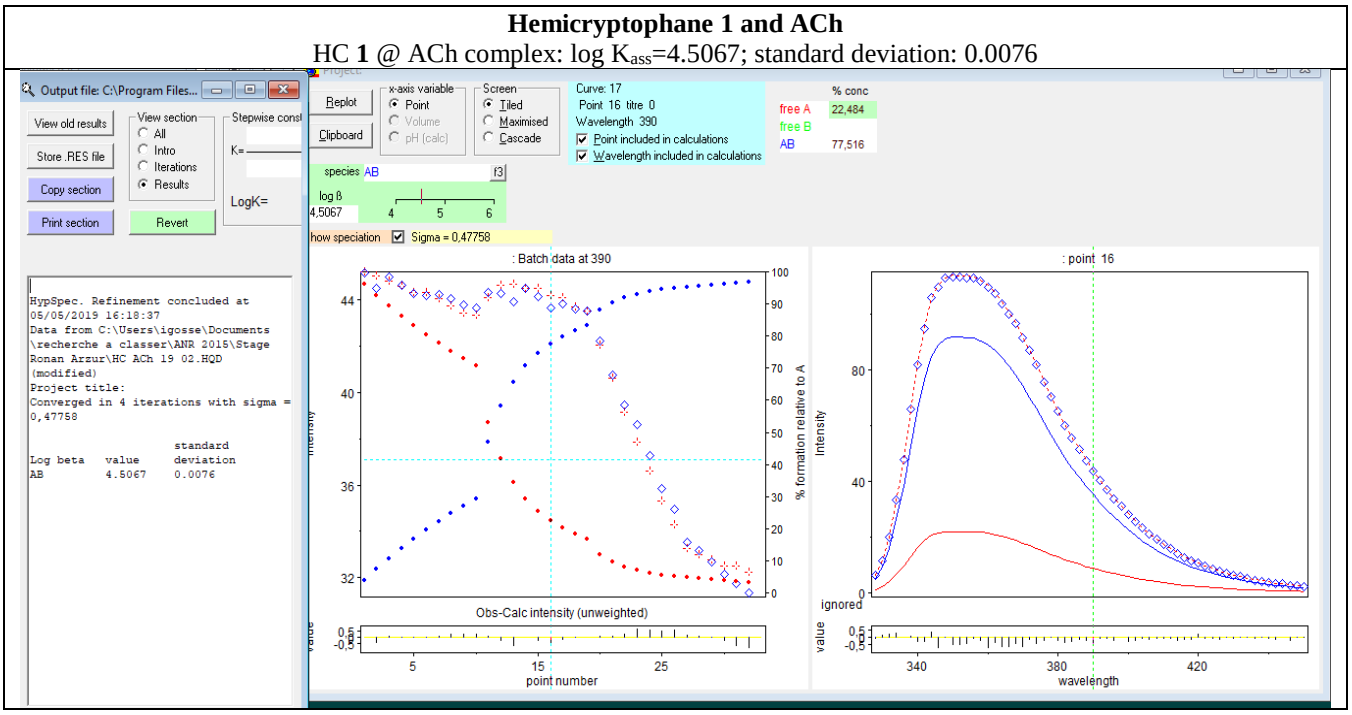

Fig. S3. Experimental data fitting of titration curves.
Figures were exported from HypSpec® program. Blue rhombuses are experimental points and the red crosses are the fitting points. Blue and red points are respectively complex and free hemicryptophane concentrations.

4. ^{1}H NMR Titrations

A solution of hemicryptophane host **1** (10^{-3}M in $CDCl_3$, 500 µL) was titrated in NMR tubes with 5 µL aliquots of concentrated solutions of acetylcholine chloride (10^{-2}M and 10^{-1}M in $CDCl_3$).

Black and red arrows visualize the evolution of host and guest NMR signals, respectively.

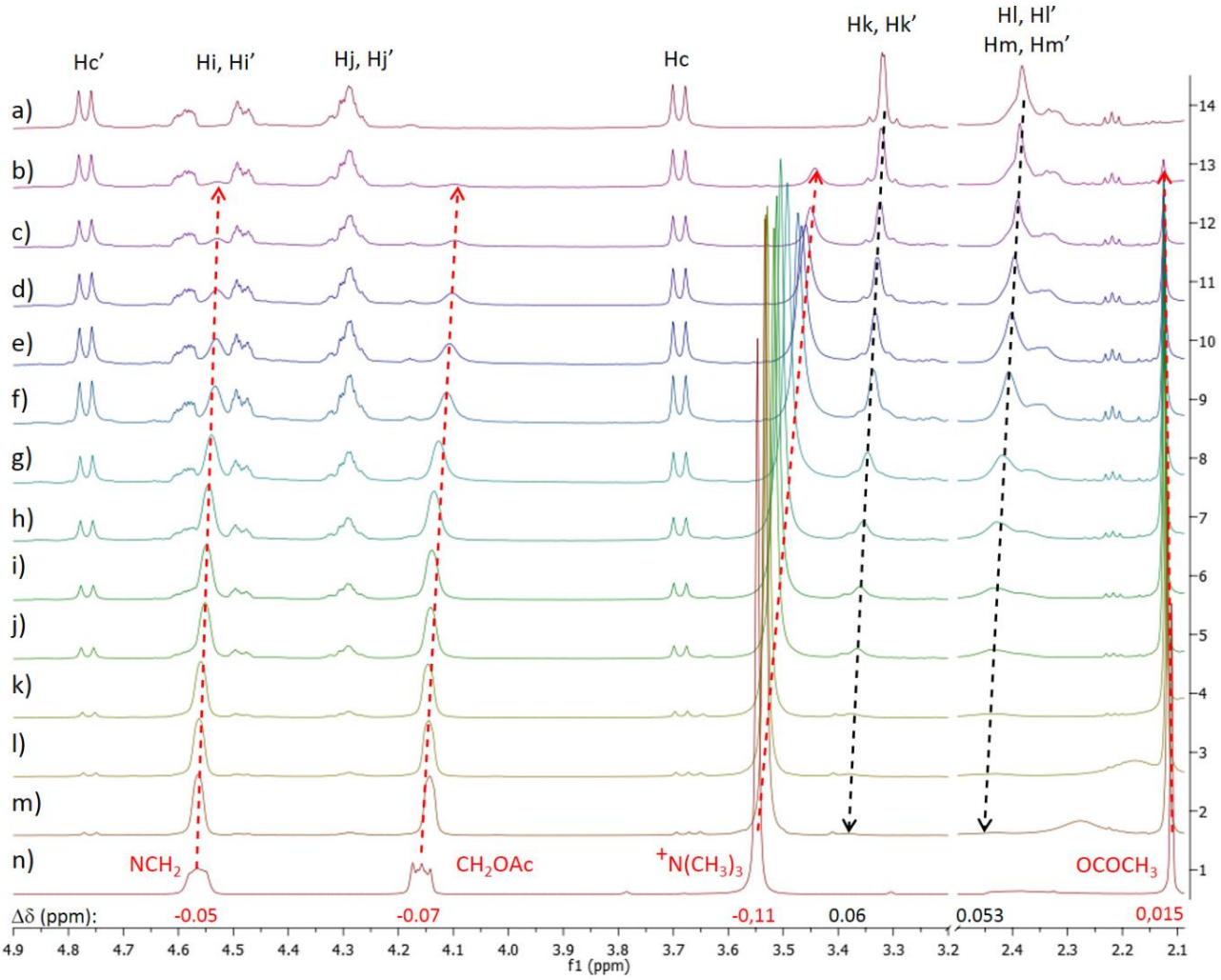

Fig. S4. ^{1}H NMR titration experiments of HC **1** in the presence of increasing amounts of ACh ($CDCl_3$, 600 MHz, 298K). Spectra (2.1-4.9 ppm domain) of pure HC **1** (a) and pure ACh (n). Spectra of HC **1** in the presence of x eq. of ACh, for x = 0.2 (b), 0.4 (c), 0.6 (d), 0.8 (e), 1 (f), 2 (g), 3 (h), 4 (i), 5 (j), 10 (k), 15 (l) and 20 (m).

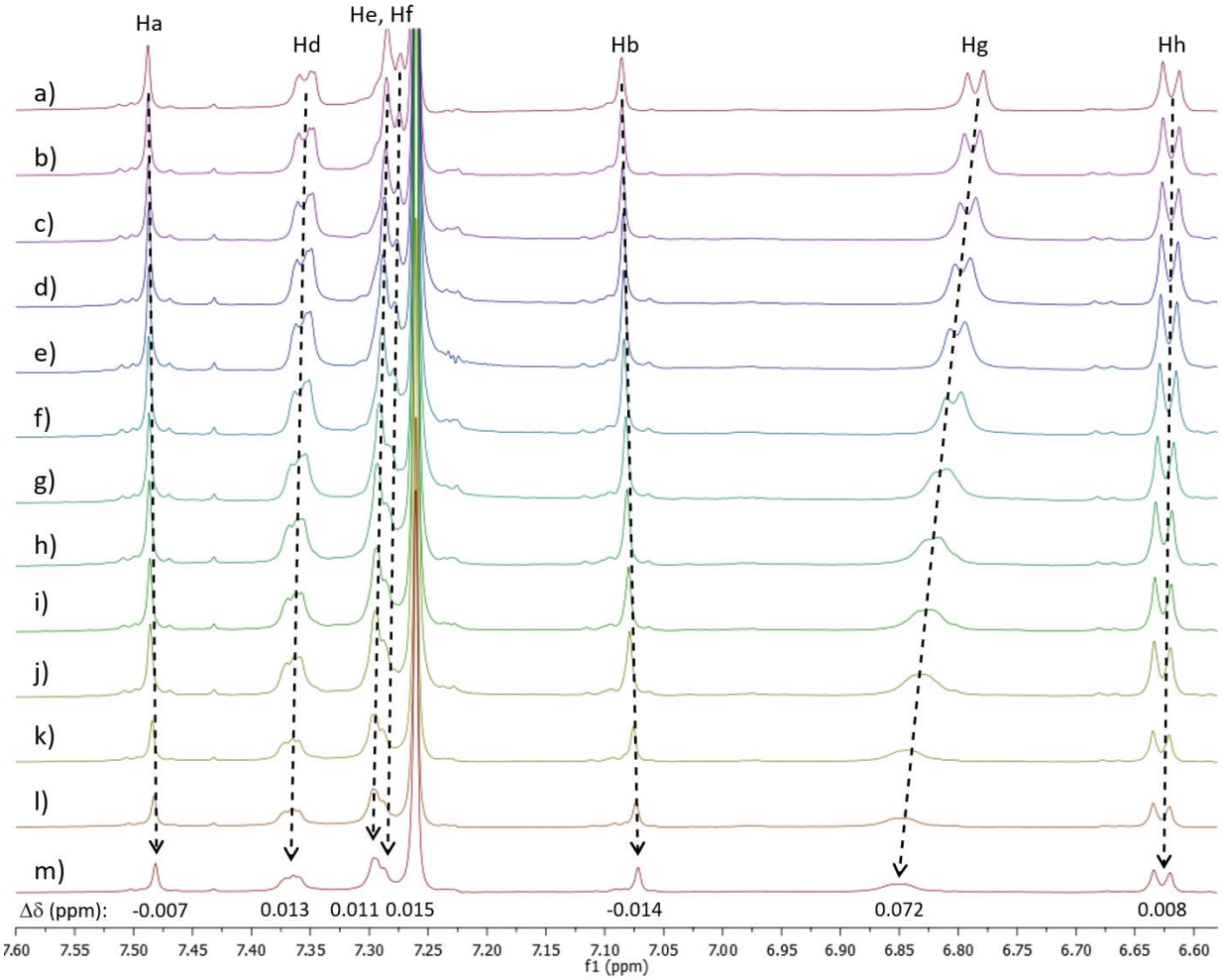

Fig. S5. ^{1}H NMR titration experiments of HC **1** in the presence of increasing amounts of ACh ($CDCl_3$, 600 MHz, 298K). Spectrum (6.6-7.6 ppm domain) of pure HC 1 (a). Spectra of HC 1 in the presence of x eq. of ACh, for x = 0.2 (b), 0.4 (c), 0.6 (d), 0.8 (e), 1 (f), 2 (g), 3 (h), 4 (i), 5 (j), 10 (k), 15 (l) and 20 (m).

5. Computational studies

Figures S6, S7 and S8 provide visualization and measurements of the relevant π-π interactions between fluorescent aromatics (in yellow) and aromatics from the hemicryptophane arms (in light blue). Figure S9 displays overlays of the cages when modelled empty (in light blue) and filled (in orange) which highlights the structural changes around the aromatic centres. In Figure S9 the conformation obtained with the acetylcholine ammonium pointing towards the CTV moiety is represented in side and top views. This conformation is found to be around 20 kcal.mol^{-1} less stable than the one discussed earlier and in the main text, with the ammonium pointing towards the TREN part.

In Fig. S10, S11 and S12 further representations of the most stable conformation, with the acetylcholine ammonium pointing towards the TREN, highlight respectively the interaction of the ammonium's nitrogen atom with phenoxy rings (Fig. S10), the hydrogen bonding between the guest and a nitrogen atom from the TREN (Fig. S11) and two additional hydrogen bonds involving oxygen atoms from the carbonyl of the Ach on one hand and from an ethylenedioxy chain on the other hand (Fig. S12).

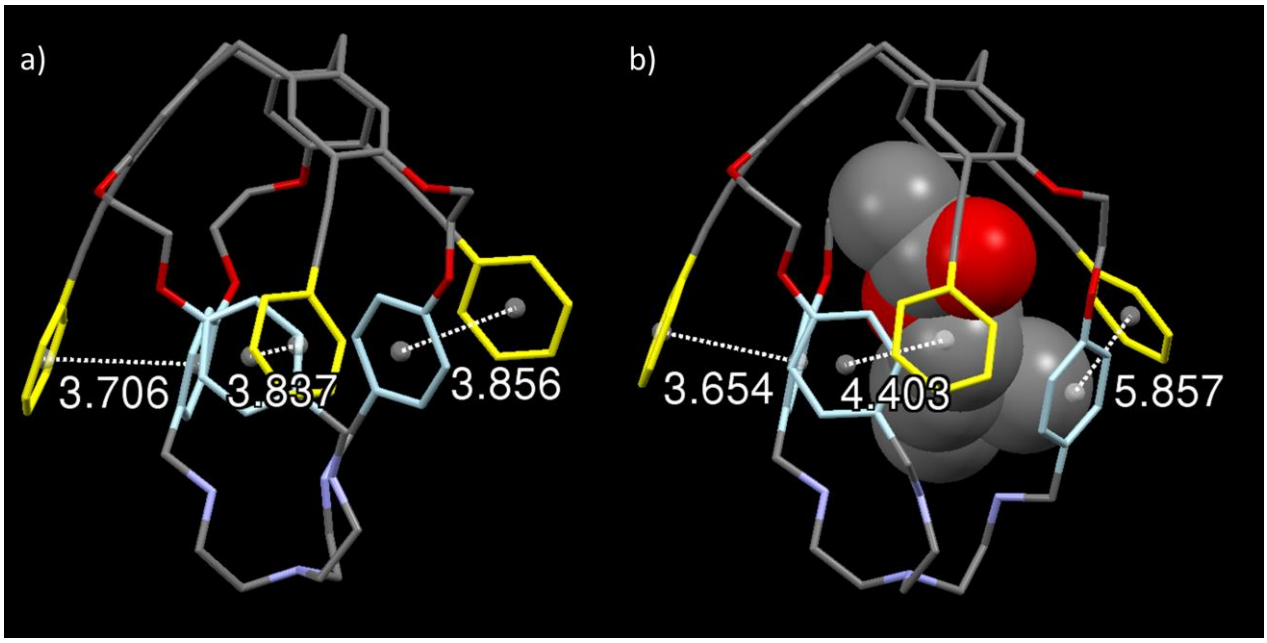

Fig. S6. DFT structure of hemicryptophane HC **1** – a) without and b) with acetylcholine. Colors are used to help differentiate the aromatic rings of alkynylbenzene units (in yellow) from those from HC **1** arms (in light blue). π-π interactions are displayed by centroids to centroids measurements with distances in Å.

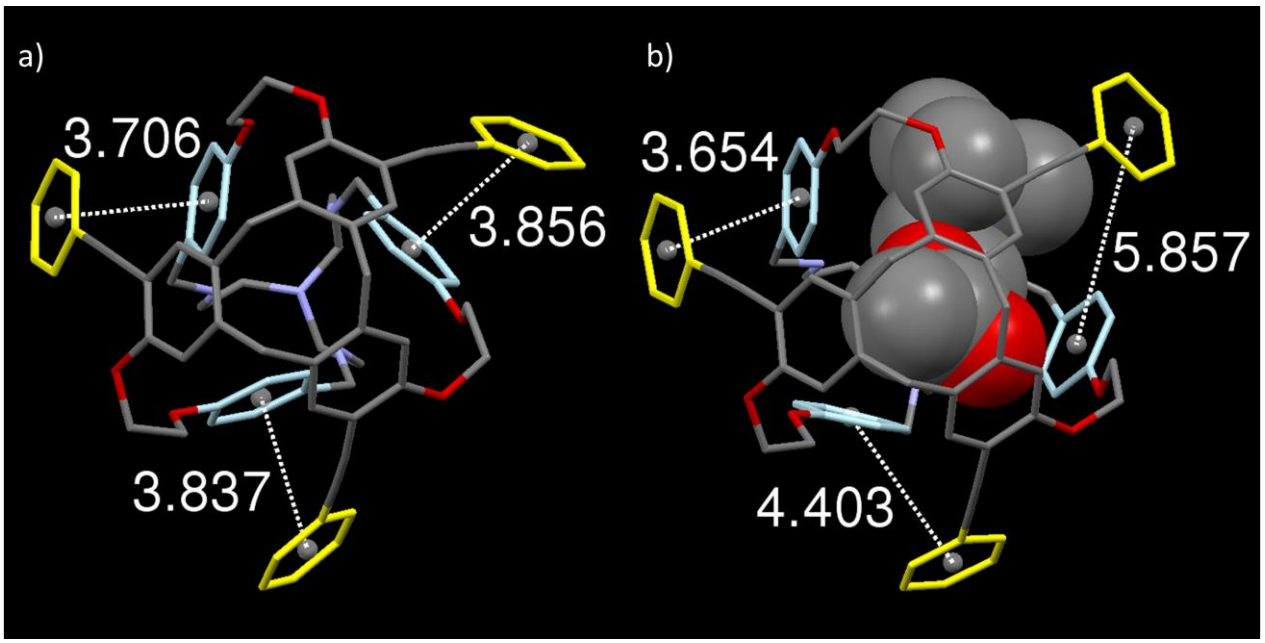

Fig. S7. Same as Figure S6 seen from above the cyclotriveratrylene unit.

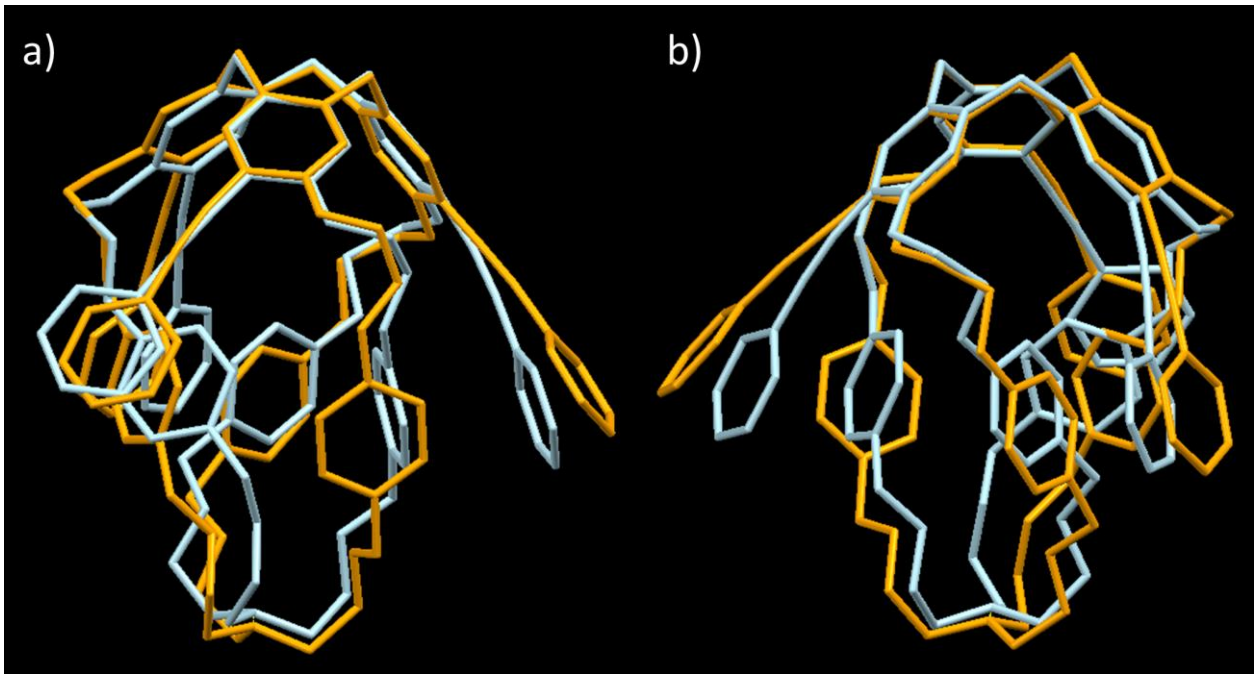

Fig. S8. Overlays of the cage structures obtained when modelled empty (in light blue) and with guest (in orange). a) and b) are two different orientations of the same thing to better illustrate the major changes. For clarity, both hydrogen atoms and acetylcholine guest are not represented.

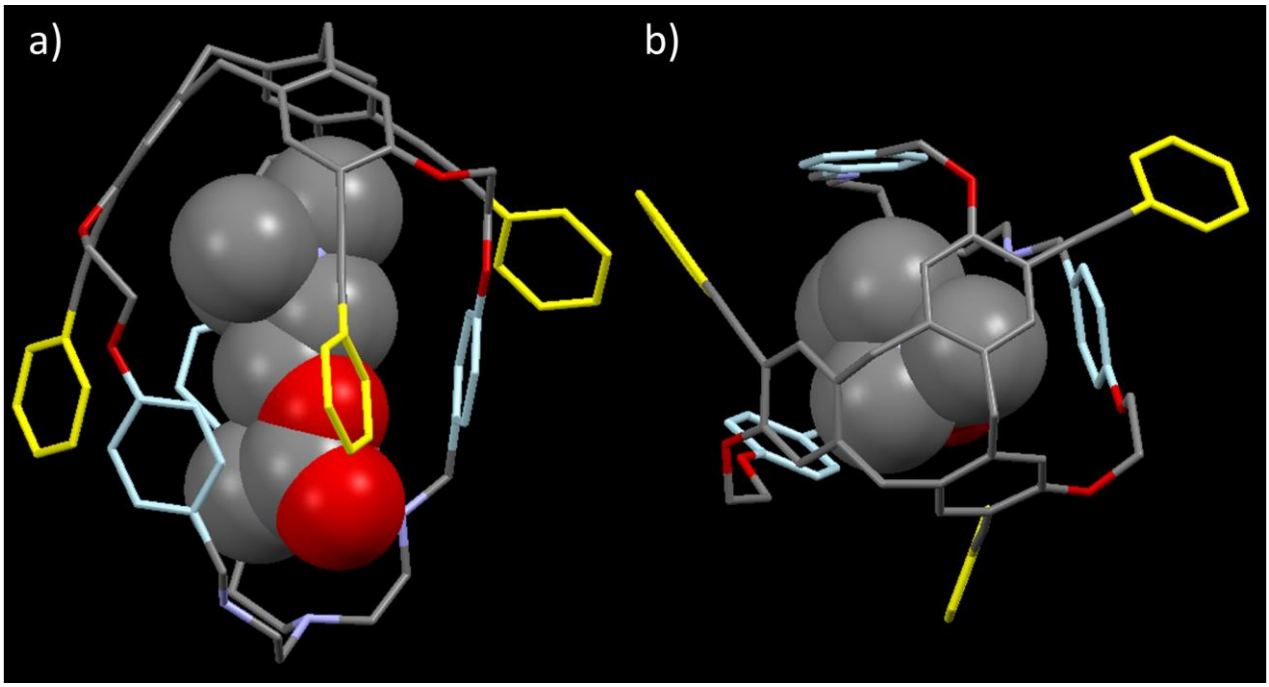

Fig. S9. a) Side and b) Top views of the DFT structure of the hemicryptophane HC **1** optimized with acetylcholine guest orientated with the ammonium pointing towards the CTV moiety.

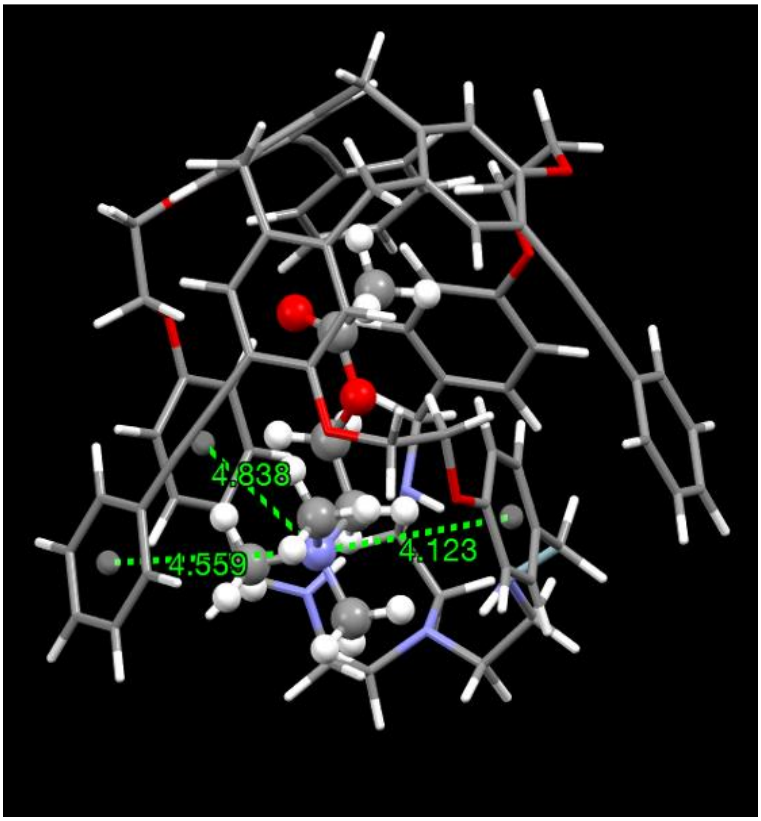

Fig. S10. DFT most stable conformation with the ammonium of the ACh pointing towards the TREN. Centroids have been calculated to represent, show and measure the π-cation interactions between the ammonium's nitrogen atom and the phenoxy rings. Distances are displayed in Å. ACh guest is represented with ball-and stick style while the host is represented with capped sticks.

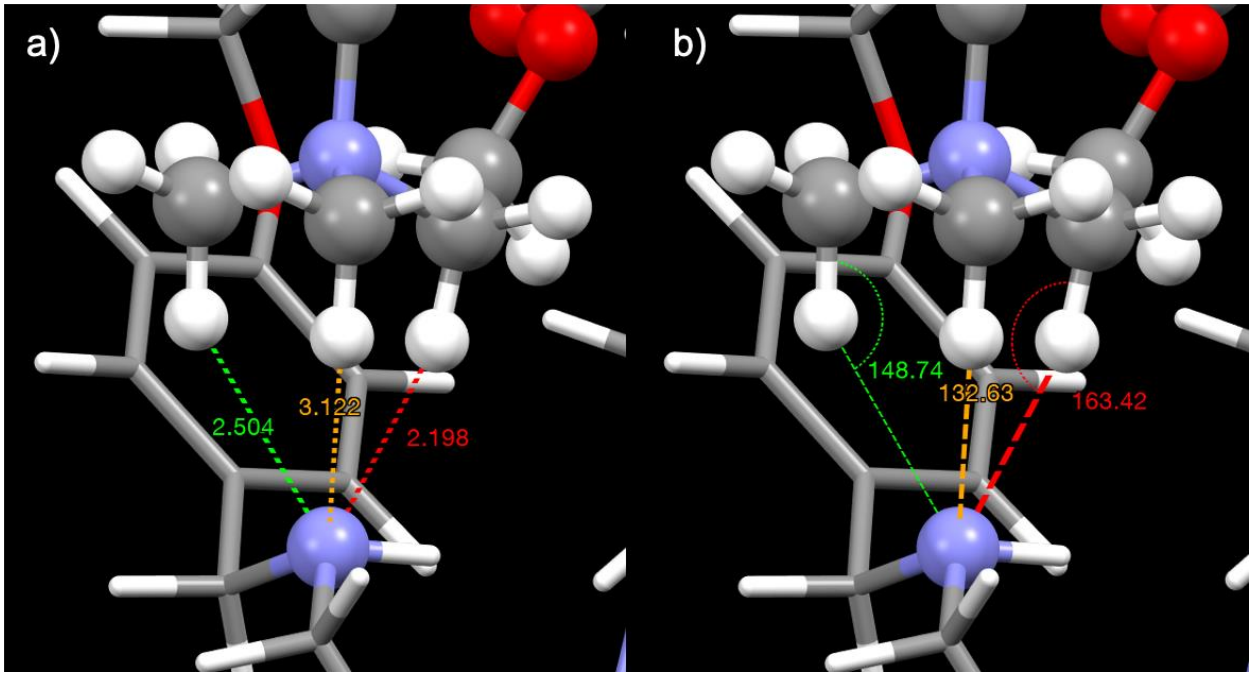

Fig. S11. DFT most stable conformation with the ammonium of the ACh pointing towards the TREN. Hydrogen bonding between the guest and a nitrogen atom from the TREN are shown with distances (in Å) displayed in panel a) and angles (in degrees) in panel b). ACh guest and the nitrogen atom involved in the interaction are represented with ball-and stick style while the rest of the host is represented with capped sticks.

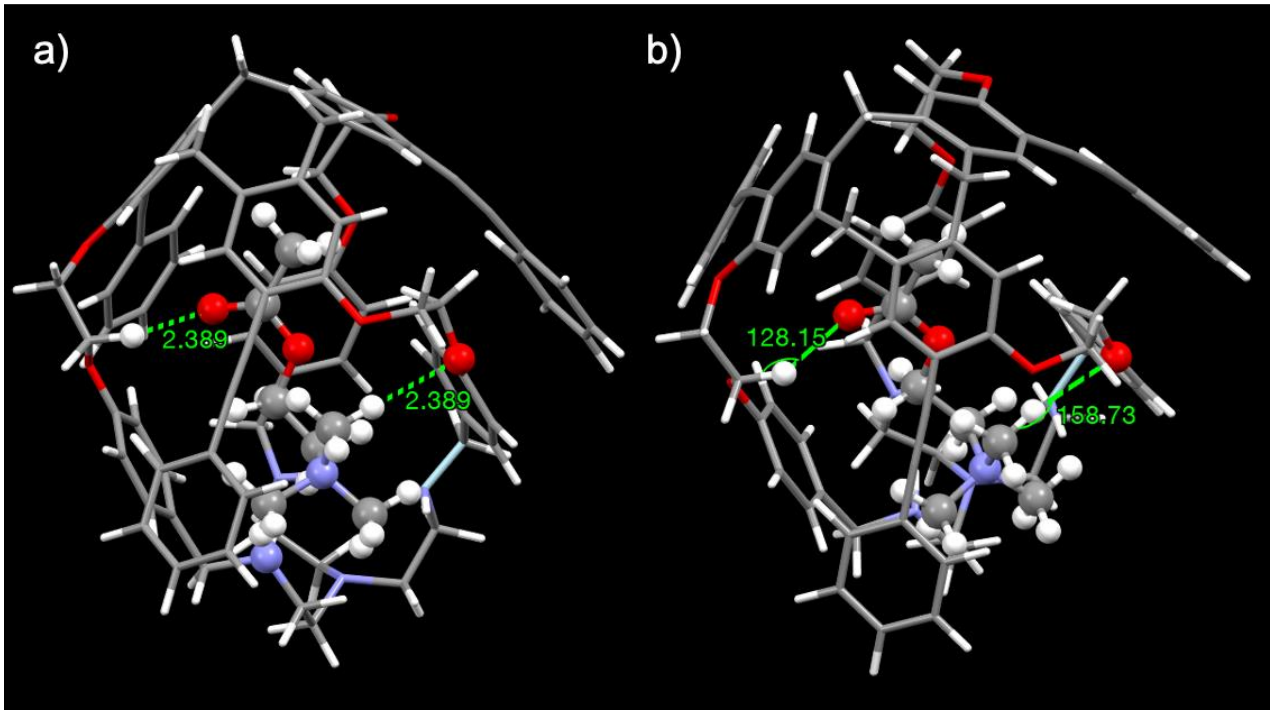

Fig. S12. DFT most stable conformation with the ammonium of the ACh pointing towards the TREN. Hydrogen bonds involving oxygen atoms from the carbonyl of the ACh on one hand (left side of each panel) and from an ethylenedioxy chain on the other hand (right side of each panel) are shown with distances (in Å) displayed in panel a) and angles (in degrees) in panel b). ACh guest and oxygen atoms involved in the interaction are represented with ball-and stick style while the rest of the host is represented with capped sticks.

6. References

[1] Brouwer, A. M. *Pure Appl. Chem.* 2011**, 83**, 2213.

[2] P. Gans, A. Sabatini, A. Vacca, HypSpec, 2008. http://www.hyperquad.co.uk.

[3] L. Peyrard, M.-L. Dumartin, S. Chierici, S. Pinet, G. Jonusauskas, P. Meyrand, I. Gosse, *J. Org. Chem.* 2012, **77**, 7023.